Improving the energy efficiency of Li-oxygen batteries by integrating the photo-catalyst

September 2017

Liu Yang

Improving the energy efficiency of Li-oxygen batteries by integrating the photo-catalyst

Graduate School of Systems and Information Engineering

University of Tsukuba

September 2017

Liu Yang

ABSTRACT

The lithium-oxygen (Li-O$_2$) battery is currently the subject of intense investigation as significantly higher gravimetric energy density ($\sim$ 3500 Wh kg^{-1}) than conventional Li-ion batteries. Moreover, the use of inexhaustible source of oxygen from ambient air makes it more attractive for widespread applications. Despite their promise, the practical achievement of rechargeable Li-O$_2$ batteries still face a lot of challenges, such as poor cycle life and rate capability, electrolyte instability and low round trip efficiency. At the center of thest drawbacks is the high charge overpotential; Recent studies have shown that the formation of Li$_2$O$_2$ particles during discharge exhibits a plateau voltage of 2.7 V, while the electrochemical oxidation of Li$_2$O$_2$ on charge typically requires voltage up to 4-4.5 V. Considerable efforts have been devoted to reduce the high charge overpotentials.

To further decrease the charge overpotential, we propose and realize the photoassisted chargeable Li-O$_2$ battery by integrating a redox coupled photocatalyst into the oxygen electrode to utilize the photovoltage during the charge process. Upon charging under illumination, the photovoltage generated on the g-C$_3$N$_4$ photocatalyst is used to compensate the required charging voltage. By integrating the g-C$_3$N$_4$ photocatalyst, an ultralow charging voltage of 1.9 V can be achieved, which is much lower than that of any other conventional nonaqueous Li-O$_2$ batteries. It should be noted that the charge voltage is even lower than the redox potential of O$_2$/Li$_2$O$_2$ (2.96 vs. Li$^+$/Li), which is thermodynamically impossible without the solar energy absorption. Such a low charge voltage dramatically elevates the electric energy efficiency to 142% (calculated based on output electric energy/input electric energy). The photo-assisted charge process offers a promising strategy for addressing the challenge of high charge overpotential in nonaqueous Li-O$_2$ batteries. In the meanwhile, the resulted low charge overpotential would alleviate the side reactions associated with carbon-based cathodes and electrolytes and elevate the electric energy efficiency of rechargeable Li-O$_2$ battery.

Based on our former research, we further continue with the study on photo-assisted Li-O_2 batteries. Although the redox mediators (RM) played a key role in reducing the charge overpotential, the side reactions and serious shuttle effect have been demonstrated. Hence, we further demonstrated an unmediated photoelectrochemical oxidation method without using any RM. With a proper design of the g-C_3N_4-carbon paper cathode, the direct photo-oxidation between photoexcited holes and Li_2O_2 discharge products can be realized. As a result, the Li-O_2 exhibits a low charging voltage of 1.96 V and favorable cycling performance by the unmediated photoelectrochemical approach. These encouraging results represent an attractive direction for the further design of photocharging all-solid-state batteries.

The lacking success of solid-state Li-O_2 battery would be attributed to the unfavorable charge overpotential derived from solid electrode-electrolyte interface. According to our previous results, the integration of solar energy can efficiently reduce the charge overpotential of Li-O_2 battery since the absorbed solar energy can be used to compensate the battery's electric energy. Owing to the better photo/thermo stability of solid electrolyte, the integration of a photocatalyst with solid-state Li-O_2 battery would be an effective strategy to reduce the severe polarization of solid-state Li-O_2 battery. In this regard, ZnS@CNT composite was synthesized and used as both an oxygen electrode and a photoelectrode. Thus the oxygen evolution reaction (OER) is greatly facilitated by photocarriers from ZnS photocatalyst, improving the charge transport within the solid-solid interface. Utilizing solar energy enables the solid-state Li-O_2 battery with a low charge voltage of 2.08 V and high electric energy efficiency of 113%, implying the critical role of solar-driven oxidation process of Li_2O_2. Thanks to its inherent advantage of high plasticity, a flexible photoassisted-solid-state Li-O_2 battery has been fabricated, which demonstrated the feasible application of our proposed solid-state Li-O_2 battery on flexible/wearable electronic devices. The solar-driven charge process provides an alternative way to improve the poor energy efficiency caused by interfacial resistance, thus contribute to the practical achievement of solid-state Li-O_2 battery.

TABLE OF CONTENTS

LIST OF FIGURES

LIST OF TABLES

x

Chapter 1 General introduction

1.1 Critical role of high energy-density rechargeable batteries

It is well-recognized that the society is becoming increasingly energy-dependent, while the extensive utilization of fossil fuels, such as oil, coal and natural gas, has led to a serious energy crisis and environmental contamination.[1] Since the majority of oil is used to power automobiles, the transition from gasoline powered automobiles to electric vehicles would do much to decrease the consumption of fossil fuels, and thereby emit fewer greenhouse gases. This is already beginning with the increasing penetration of hybrid electric vehicles in the global market, which further lead to an urgent search for renewable and clean energy sources. Because the renewable energy is intermittent in nature as a result of atmospheric conditions, without energy storage devices, the renewable energy for electricity production would become much less viable.[2; 3] Therefore, energy storage mediums play a critical role to balance the mismatch between the electricity consumption and production. Due to their good reversibility and device flexibility, electrochemical batteries show appealing potential to store the renewable energy for enabling continuous utilization. As a result, electrochemical rechargeable batteries are widely used in mobile equipment, such as cellular phones, personal computers and digital cameras.

The key properties of today's principal rechargeable batteries are listed in table 1.[4-7] Lead-acid batteries have been used for more than one century from ~1859, mainly as the power source for automotive starter. Since the year of 1899, the nickel-based batteries have experienced a period of prosperity due to the considerable demand of portable electronic devices (phones, toys etc.). The low operating voltage of lead-acid and nickel-based batteries and the heavy electrode materials finally lead to low energy density.[8] With the pursue for high energy densities, the breakthrough of Li-ion batteries has been achieved in 1991 by Sony Corporation, which delivers a specific energy as high as 160 Wh kg^{-1}.[9] Due to superior specific, long cycle life and no

memory effect, Li-ion batteries are considered as relatively new technology. Until now, LIBs still occupies the major position for use in portable electronics. Increasingly they are being scaled up for use in electric vehicles as well.

Table 1. 1. Key properties of today's principal rechargeable batteries.

System	OCV (V)	Theoretical specific energy (Wh kg^{-1})	Practical specific energy (Wh kg^{-1})
Pb-acid	2.1	171	40
Ni-Cd	1.35	219	40
Ni-MH	1.35	240	60
Li-ion	3.8	387	160
Li-ion (Si anode)	4.0	420	~200
Li-S	2.0	2567	~370
Li-Air	3.0	3505	~1700

1.1.1 The limitation of LIBs for use in electric vehicles

LIBs are widely used in many electronic devices which are very important to our daily life. While the energy density of current LIBs can hardly satisfy the energy demand for electrifying transportation, several approaches have been carried out to improve the energy density of state-of-the-art LIBs.[10] The primary cell reactions are based on reversible Li-ion intercalation/de-intercalation between cathode and anode host structures. Hence, the most important innovative steps as made for advancing this field are related to the development of electrode materials.[11; 12] From the viewpoint of cathode, lithium transition metal oxides (LiM_xO_y) have been considered as the most attractive cathode materials.
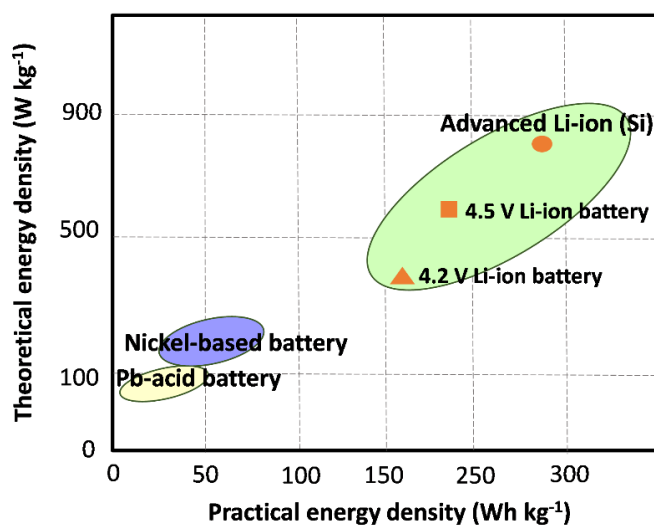
Fig. 1. 1 The development of rechargeable batterieis toward high energy densities

While the capacities of these cathode materials are still far behind the expectation for use as electric vehicle batteries (such as layered $LiCoO_2$ 140-160 mAh g^{-1}, olivine $LiFePO_4$ ~150 mAh g^{-1} spinal $LiMn_2O_4$ ~120 mAh g^{-1}). For example, one alternative approach is to elevate the operating voltage by developing cathodes with high electrochemical potential. Spinel structured $Li(Ni, Mn, Co)O_2$ offers a charge voltage up to 4.5 V, resulting in a limited improvement to 160-180 mAh g^{-1}.[13] Moreover, the high voltage batteries suffer from operational instabilities especially at high temperatures. On the other hand, extensive studies have been focused on the anode materials. After a broad exploitation of higher capacity anode materials, Silicon (Si) has emerged as a promising candidate to substitute graphite anode, which can reversibly alloy with lithium with a stoichiometry of $Li_{4.4}Si$, offering a high theoretical capacity of 4200 mAh g^{-1}.[14; 15] Unfortunately, due to the densely structure of metalloids, huge volume expansion of Li-Si anode would occur during lithiation, even up to 300% in some case. This leads to the crack of electrode particles, deteriorated electronic conductivity and further capacity fading during cycling.[16] Many strategies have been developed to alleviate the volume expansion of Li-Si anode. It is found that nano-structured Si material such as nanowire morphology, can effectively accommodate the volume change of Li–Si alloy upon lithiation. By using the nanowire Si anode, the

3

enhanced energy density of ~300 Wh kg^{-1} can be achieved.
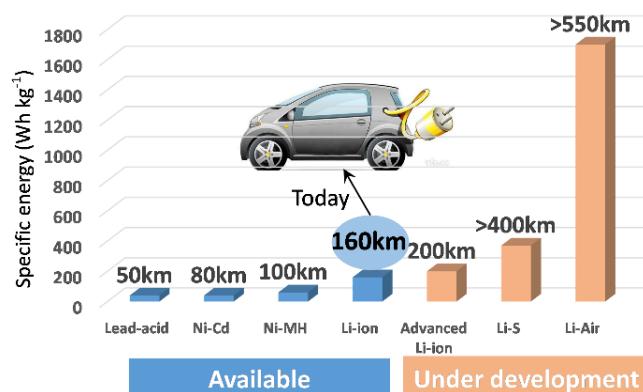
Fig. 1. 2 The estimated driving ranges for electric vehicles with various rechargeable batteries

After a steady of improvement of ~15% over the last two decades, the energy density of LIBs is currently limited by the Li$^+$ intercalation chemistry. More importantly, the energy density of LIBs is far from the goal for use in electric vehicles, even large efforts are made to improve their energy-density closed to theoretical limits. Thereby, various innovative battery system have been developed, for instance, Li-S battery and Li-polymer battery etc.[17-19] Although some hope have been shown by these advanced battery technology, technical issues still plague them.[20; 21] For instance, the so-called "shuttle effect" in Li-S chemistry is caused by dissolved polysulfides migrating to Li anode where they react. Extensive research efforts are definitely expected. With today's automotive Li-ion battery, the driving range of electric vehicles is limited to ~160 km, as shown in Fig. 1.2. More importantly, even the energy-density of Li-ion battery is further improved closed to their theoretical limit, it can hardly meet the demand for electric vehicles.[22; 23] In this case, new technologies beyond Li-ion chemistries need to be searched to meet high energy-density demand for electric vehicles. Among all chemistries beyond Li-ion, Li-Air batteries have received enormous research attention to break through the energy-density limitations. According to the Web of Science, published papers and patents in this area has increased rapidly in the last couple of years. As shown in Fig. 1.2, in theoretical, Li-air batteries have the potential to support for a

driving range ~500 km, at least 2-3 times greater than that of Li-ion batteries.[24]

1.2 Lithium-Air battery

1.2.1 Introduction of Li-air battery

Based on the various electrolyte properties, Li-air batteries can be classified into four versions, that is, nonaqueous, aqueous, hybrid and solid batteries, as shown in Fig. 1.3. Nonaqueous Li-air batteries using aprotic electrolyte were firstly introduced by Abraham and Jiang in 1996.[25; 26] Aqueous Li-air batteries are operated based on the inorganic lithium salt dissolved in H_2O solvent as the electrolyte. Wang and Zhou propose a new type Li-air batteries which is based on hybrid electrolyte with an aqueous electrolyte in cathode side and an organic electrolyte in anode side.[27] The all-solid-state Li-air batteries were reported by Kumar to improve the security assurance[28]. In the case of aqueous and hybrid $Li-O_2$ batteries, a Li protection film is of essential importance, which is designed to prevent the drastic reaction between water and Li. Aqueous and hybrid systems share the same reaction mechanisms since the oxygen electrodes are exposed to aqueous electrolytes. It is demonstrated that the maximum available energy-density of aqueous $Li-O_2$ battery is much less than that when using aprotic electrolytes [29]. Further, the non-aqueous Li-air batteries shows more simple structure similar with typical Li-ion batteries, except the system is open to absorb O_2 gas. The working principle in all-solid-state Li-air battery is similar to the nonaqueous system. However, it is not widely investigated primarily due to the low ionic conductivity of solid electrolyte and large interfacial resistance. During my Ph.D. period, I mainly focused on the aprotic $Li-O_2$ system since it has dominate the development of this research field.
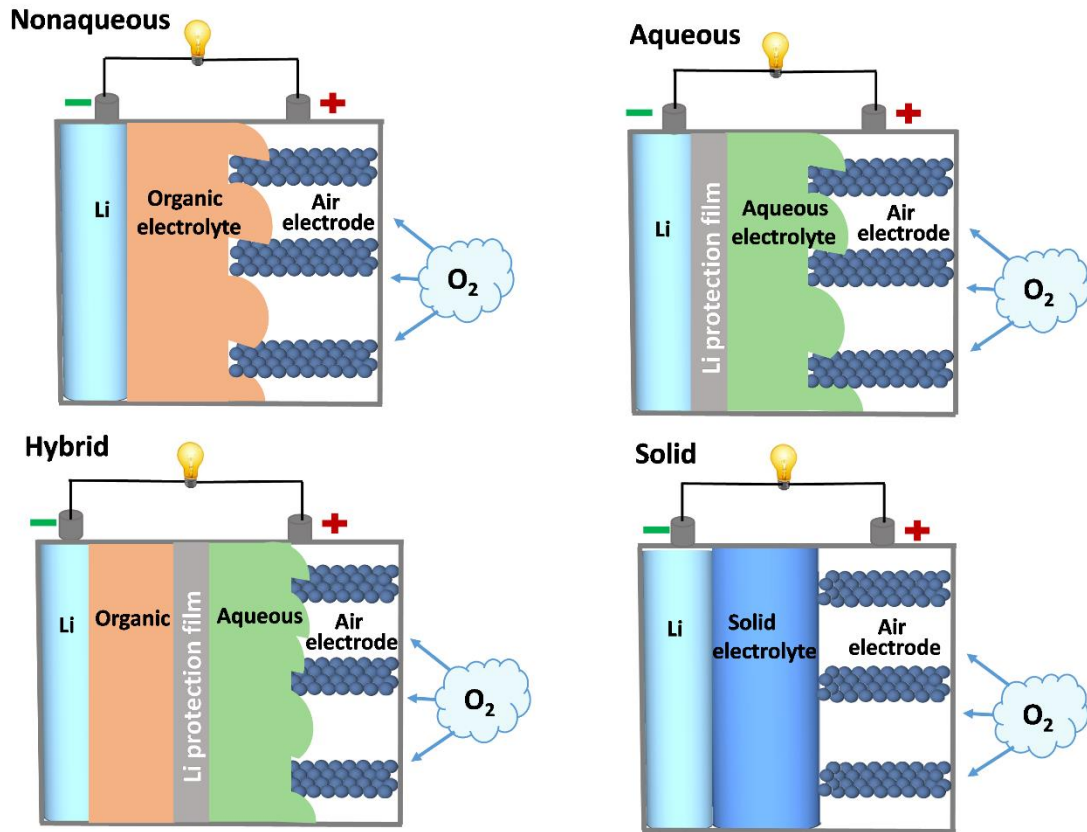
Fig. 1. 3 Four principal Li-air battery configurations.

1.2.2 Working principle of Li-air battery

A non-aqueous Li-air battery typically consist of a lithium metal anode, a Li^+ conductive electrolyte and a porous cathode. $Li-O_2$ batteries operate based on simple reaction between Li^+ and O_2 with a thermodynamic potential of 2.96 V : $2Li^+ + 2e^- + O_2 \leftrightarrow Li_2O_2$.[30] The schematic diagram of working principle during discharge/charge process is given in Fig. 1.4. During discharge process, O_2 molecules enters the pores of cathode, and reduced by electrons from the current collector to combine with Li^+ to produce Li_2O_2 on the cathode. Subsequent charge causes a reverse reaction, making the $Li-O_2$ battery to be rechargeable. Upon charge process, these Li_2O_2 particles are electrochemically decomposed to release Li^+ and O_2 gas.[31] A porous cathode is particularly necessary since it not only allow the diffusion of O_2 but also provide the space to store Li_2O_2 product. The capacity of a $Li-O_2$ battery is determined by the pore

space in cathode for the storage of Li_2O_2 products. Thus extensive research activities have been dedicated on the cathode materials. Due to the inherent advantages of lightweight, high conductivity and large surface areas, carbon-based materials has been chosen as the cathode materials for most of the $Li-O_2$ batteries. In addition, carbon materials have exhibited certain catalytic activity toward oxygen reduction reaction. Various carbon materials have been widely used in current Li-air batteries including commercial carbon black, carbon nanotubes, graphite and carbon fibers etc.[32-34]
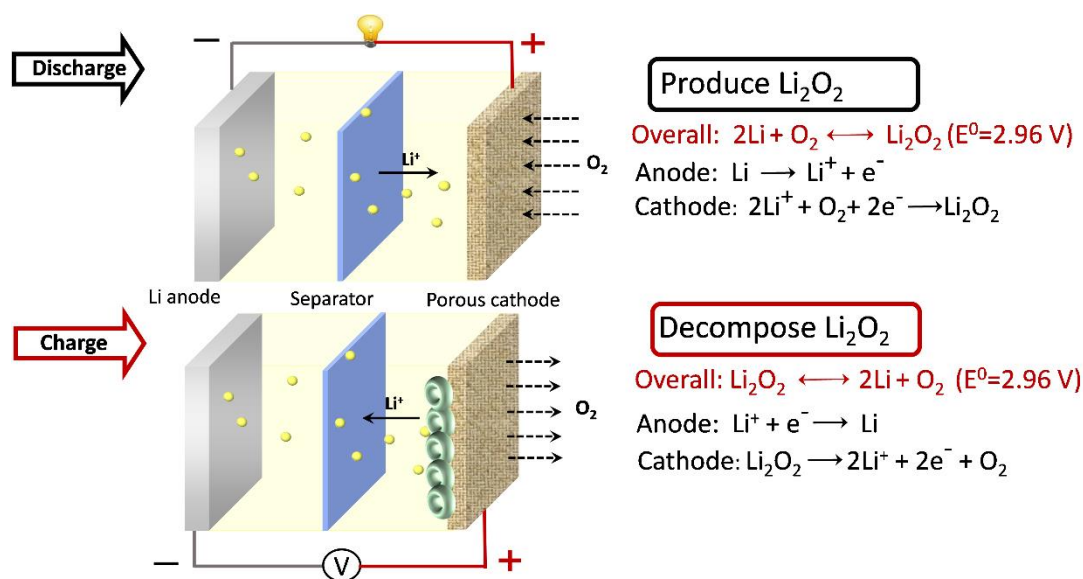
Fig. 1. 4 The schematic of working principle for nonaqueous Li-air batteries.

1.3 Major challenges in current $Li-O_2$ batteries

Although the $Li-O_2$ chemistry possess the greatest theoretical energy-density (~3550 mAh g^{-1}), this promising technology has been hindered by several critical challenges, such as electrolyte instability, poor cycle life and low round-trip efficiency.[35] These drawbacks are mainly caused by the high overpotential issue during charge process.

1.3.1 High charge overpotential issue

The typical discharge/charge profiles of non-aqueous $Li-O_2$ battery is presented in Fig. 1.5. In practical, $Li-O_2$ battery usually exhibit a discharge voltage around 2.7 V, which is coincident with an equilibrium voltage of 2.96 V. While large overpotentials

are found during charge process, as much as 4.0 V in some case.[36; 37] The high overpotential directly lead to following issues: (1) It is demonstrated, at high voltage (> 3.5 V), carbonate-based electrolyte (such as EC/DEC and PC) are readily attack by the intermediate O_2^- species, yielding undesired products such as Li_2CO_3.[38] As an alternative, ether-based electrolytes (that is, non-carbonate electrolytes) are considered more stable than carbonate-based electrolytes, although the decomposition remain at high voltage (> 3.5 V).[25; 39-41] (2) Side reactions between carbon-based cathode and Li_2O_2 and decomposition of carbon cathode itself severe polarization (3) poor cycling life[34; 42] (4) low energy efficiency around 60% (output electric energy/ input electric energy).[43] This value is unacceptable low for use as a practical energy storage system. The high charge overpotential could be attribute to the insulating and nonconductive nature of Li_2O_2, thus its electrochemical decomposition requires high charge voltage.[44; 45] In addition, the pores in air electrode are easily clogged thus the diffusion of Li^+ and O_2 are blocked, causing further overpotential.[46] More seriously, the decomposition of electrolyte and carbon-base electrode could directly lead to the formation of Li_2CO_3 byproduct. These side products can't be fully removed without climbing to high voltage which, in turn, accelerate the high charge overpotential issue.[47] Due to the presence of high charge overpotential, the OER process seems to be more critical than ORR process to realize a reversible Li-O_2 battery.
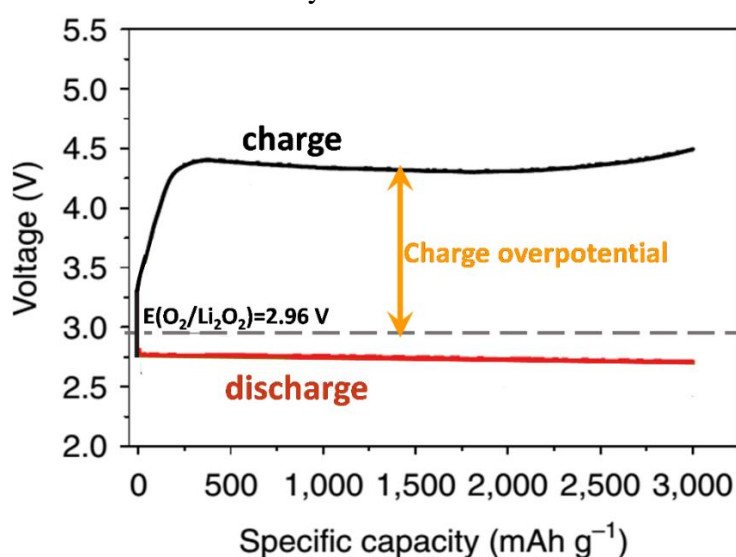
Fig. 1. 5 A typical discharge/charge profile of non-aqueous Li-O_2 battery

1.3.2 Strategies to reduce the charge overpotential

Reducing the charge overpotenial are indispensable to insure the battery component stable and enhance energy efficiency. Thereby, considerable efforts have been devoted to address the severe charge overpotential issue and two approaches are generally used. One alternative solution is to construct highly active electrochemical catalysts toward OER and ORR processes. Transition metal and oxides (Co_3O_4, MnO_2, TiC and TiN) and precious metal and oxides (Pt, Au, Ru and RuO_2 etc.) are widely investigated as electrocatalysts for $Li-O_2$ battery. Earlier studies demonstrated that the electrochemical catalyst could efficiently increase the kinetics of Li_2O_2 decomposition on charge. Further, these catalysts supported on carbon-based materials are extensively attempted and show increased catalytic activity. We summarize some recent reported work on electrochemical catalyst and the obtained performance was listed in Table 1.2.

Table 1.2. Summary of the performance improvement of non-aqueous Li-air battery with electrochemical catalyst.

Cathode materials	Voltage (V)	Specific capacity (mAh g^{-1})	Cycle life	Ref.
Pt/C	~ 3.8	750	/	[48]
Au/C	~ 4	1500	/	[48]
PtAu/C	~ 3.6	1300	/	[49]
Pt/MnO$_2$	~ 3.5	150-250	20	[50]
Ru/ITO	~ 3.6	2.5 mAh cm^{-2}	50	[51]
RuO$_2$/CNT	~ 3.5	1800	20	[52]
RuO$_2$/CNF	~ 3.6	20600	300	[53]
Pd/Al$_2$O$_3$/C	~ 3.3	> 1000	10	[54]
α-MnO$_2$	> 4.0	2300	10	[55]
Nanoporous Au	~ 3.5	330	100	[56]
Pd/MnO$_2$	~ 3.6	550	15	[57]
RuO2/rGO	~ 3.6	> 5000	30	[58]

MoN/NGS	~ 4.0	1490	9	[59]
CoMn$_2$O$_4$/GNS	~ 4.0	3000	7	[60]
Fe/N/C	~ 3.6	450	50	[61]
TiN/C	~ 3.8	6000	/	[62]
Co$_3$O$_4$/Carbon sphere	~ 4.0	7000	/	[63]
Co$_3$O$_4$/HGPC	~ 3.55	500	50	[64]
Mo$_2$C/CNT	3.25-3.4	500	100	[65]
La$_{0.75}$Sr$_{0.25}$MnO$_3$/KB	~ 3.9	1000	130	[66]
La$_{0.5}$Ce$_{0.5}$Fe$_{0.5}$Ni$_{0.5}$O$_3$/GNS	~ 3.8	1100	100	[67]
Pyrochlore	~ 3.8	8000	4	[68]

Another alternative approach is to incorporate a redox mediator (RM) into electrolyte to reduce the charge overpotential.[69] The diffusible RM could easily move around in the electrolyte and have sufficiently wet contact with Li$_2$O$_2$ discharge products. The reaction mechanism is one in which RM are initially oxidized to the oxidative form of M^{ox} during charge process. Subsequently, the oxidized reactors M^{ox} chemically react with Li$_2$O$_2$ particles, producing Li$^+$ and O$_2$ gas. At the same time, by oxidizing Li$_2$O$_2$ the M^{ox} is reduced back to M^{red}.[70] RM as diffusible catalyst in Li-O$_2$ battery has to fulfill several conditions. (1) The redox potential should be compatible with that of Li$_2$O$_2$ products formation. In other words, the oxidative potential of RM is required to be higher than the redox potential of Li$_2$O$_2$ formation. (2) The oxidation form of RM should be capable of oxidizing Li$_2$O$_2$ particles. (3) The redox mediator must not react with the electrolyte and Lithium anode. In addition, it should be highly dissolved in the electrolyte. Based on the above-mentioned conditions, many redox-active molecules have been successfully attempted in Li-O$_2$ batteries, such as tetrathiafulvalene (TTF), ferrocene (FC) and N,N,N′,N′-tetramethyl-p-phenylenediamine (TMPD). The

summary of performance improvement of non-aqueous Li-O$_2$ batteries with various redox mediators are presented in Table. 1.3.

Table 1.3. Summary of the performance improvement of non-aqueous Li-O$_2$ batteries with redox mediators

Redox mediator	Redox potential (V)	Specific capacity (mAh g^{-1})	Cycle life	Reference
Ferrocene (FC$^-$/ FC)	3.60	/	/	[71]
OMAB$^-$/OMAB	3.16	1000	/	[72]
TMPD$^-$/TMPD	3.33	500	50	[71]
Lithium nitrite (LiNO$_3$)	3.6	1000	50	[73; 74]
I$_3^-$/I$^-$	3.05	1000	900	[75; 76]
(FePc)$^-$/ (FePc)	3.55	1000	135	[77]
Tetrathiafulvalene TTF	3.56	300	100	[71; 78; 79]
2,2,6,6-Tetramethylpiperidinyloxyl (TEMPO$^+$/ TEMPO)	3.74	500	/	[80; 81]
Cesium iodide (CsI)	3.6	1500	125	[82]
Tris[4-(diethylamino)-phenyl]amine (TDPA)	3.4	500	100	[83]

1.3.3 Safety hazards derived from organic liquid electrolyte

The Li-O$_2$ batteries have gained extensive interest due to the potential application for electrifying transportation. However, there are still many fundamental and technical problems associated with Li-air batteries. Among these, some intrinsic problems are arisen from the use of organic electrolytes. During discharge process, Li$_2$O$_2$ forms on

the air electrode by a stepwise type: $O_2 \rightarrow O_2^- \rightarrow O_2^{2-}$. The O_2^- as supernucleophile could readily attack the organic electrolyte, resulting in the formation of Li_2CO_3 byproduct.[32; 84] More seriously, the use of combustible organic electrolyte encounters safety issues.[85; 86] That is, the combustible, flowing and volatile natures of the organic liquid electrolytes cause safety issues such as leakage, fire and even explosion.[87] These issues are becoming more serious with the increasing size of batteries used in electric vehicles. In this regard, developing solid-state Li-air batteries has been studied as the safest and the most reliable concept. Various solid electrolytes have been developed to replace the organic electrolytes, such as inorganic solid electrolyte, polymer electrolyte and ceramic electrolyte.[88-90] Using solid electrolyte also has the advantage that the lithium anode can be protect toward air by the solid electrolyte layer. Currently, most studies on Li-air batteries have employed pure O_2 atmosphere rather than air to avoid unwanted side reactions with components in ambient air (H_2O, CO_2). Namely, the dense solid electrolyte has the potential to prevent the corrosion by water and CO_2. While the further advance of solid-state Li-air battery has been restricted by low ionic conductivity, Li ion transfer number and large interfacial resistance. As a result, the cycling life and rate capability of these solid systems remains inferior.

1.4 Target and outline of this dissertation

1.4.1 Research purpose

Although many research efforts have been dedicated to reducing the charge overpotential, the obtained results are still far from satisfactory, and the energy efficiency of Li-air battery requires to be improved. The OER process plays the most critical role in the operation of Li-O_2 battery and determine whether a rechargeable Li-O_2 battery can be achieved.[43] By the conventional strategies (i.e. RM, electro-catalyst) to reduce charge overpotential, the charge potentials are still as high as 3.5- 3.7 V. This directly lead to low electric energy efficiency around 60% (calculated based on output electric energy/ input electric energy), indicating that the input electric energy far

exceeds output electric energy. In the Li-O$_2$ battery with redox mediator, the charge voltage is determined by the redox potential of M^{red}/M^{ox} since the charge process is achieved by the chemical reaction between redox mediator and Li$_2$O$_2$, as shown in Fig. 1.6.
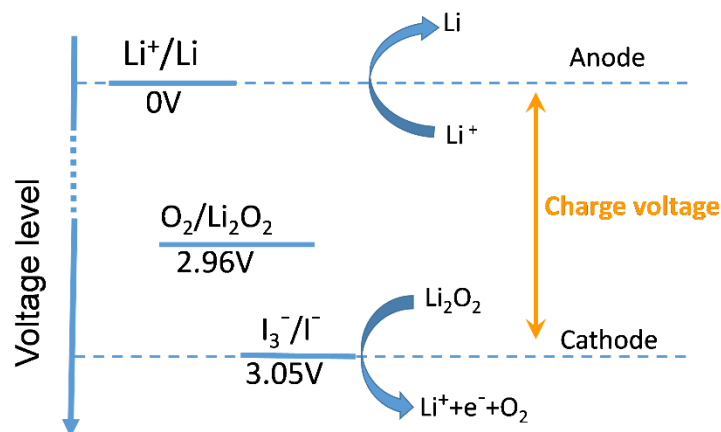
Fig. 1. 6 Energy diagram of non-aqueous Li-O$_2$ battery with LiI redox mediator

Therefore, we attempt to introduce photocatalyst in air elelctrode to capture solar energy into Li-air battery. For this proof-of-concept, we employ the g-C$_3$N$_4$ photocatalyst coupled with redox mediator to construct the photo-assisted Li-O$_2$ battery. In our photo-assisted battery, the discharge process is same with that of a conventional battery. While during charge process, the electrochemical conversion of M^{red}/M^{ox} is gained by photoexcited holes oxidation (seen in Fig. 1.7). In other words, upon charging under illumination, photoexcited electron-hole pairs would generated on the g-C$_3$N$_4$ photocatalyst. Thus, the photovoltage would on the g-C$_3$N$_4$ photocatalyst can be used to compensate the required charge voltage. As expected, the charge overpotential issue is effectively addressed and the side reaction at high voltage can be suppressed. This photo-assisted charge strategy is further extended to solid-state Li-O$_2$ battery to improve electric energy efficiency.
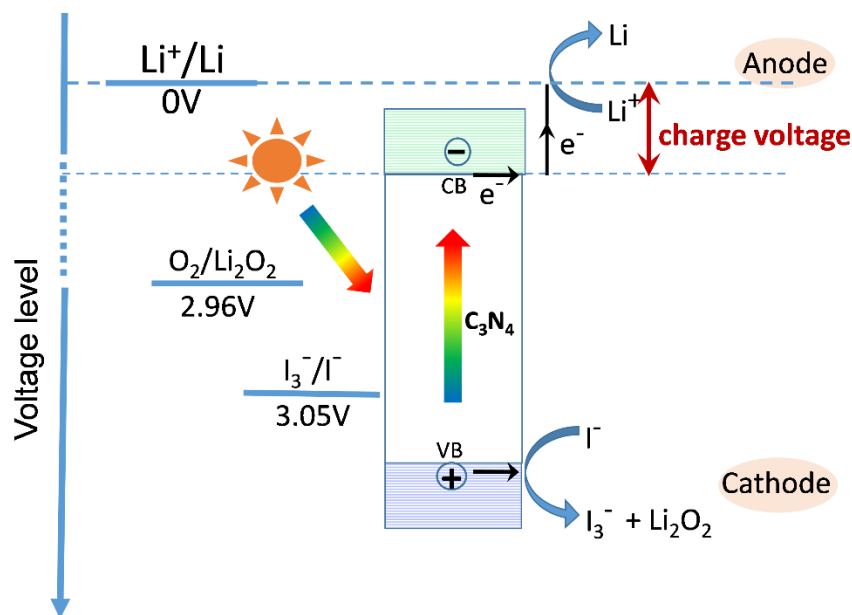
Fig. 1. 7 Energy diagram of photoassisted Li-O$_2$ battery with LiI redox mediator

1.4.2 Targets of this research

➢ To reduce the charge voltage by introducing photocatalyst into Li-O$_2$ battery

➢ To simplify the photo-assisted Li-O$_2$ battery configuration and improve cycling performance

➢ To apply the photo-assisted charge strategy in solid-state Li-O$_2$ battery for high electric energy efficiency

1.4.3 Outline of this thesis

There are five chapters in this dissertation in total.

Chapter 1 is the brief background of the research study. It mainly include the critical challenge for current LIBs, the necessity to develop high energy-density Li-air battery, a general introduction of Li-air battery, the challenges in making practical Li-air batteries and reported solutions. The research purpose and targets are also provided.

In chapter 2, a photo-assisted Li-O$_2$ battery is fabricated by employing g-C$_3$N$_4$ photocatalyst coupled with LiI redox mediator. It is noted that g-C$_3$N$_4$ acts as a photocatalyst and an oxygen reduction reaction (ORR) catalyst simultaneously. By

absorbing solar energy via g-C_3N_4, an ultralow charge voltage of 1.9 V is obtained, which is the lowest value so far, resulting in a high electric energy efficiency of 142%.

In chapter 3, based on our former research, we further continue with the study on photo-charge Li-O_2 batteries. Although the redox mediators played a critical role in reducing the charge overpotential, we discovered serious shuttle effect and side reaction related to redox mediators. Hence, we here design and realize a photo-charged Li–O_2 battery without using any RM. The overpotential issue has been effectively addressed by absorbing solar energy during charge process. The photo-charge process without redox mediators has proved to be efficient by experimental evidence together with theoretical analysis. Through this work, we improve the shortcomings in our former work, meanwhile, guide a promising avenue for the future development of photocharging all-solid-state batteries.

In chapter 4, due to solid electrolyte-electrode interface, the charge overpotential issue in solid-state Li-air battery is even more serious than that in conventional Li-air battery. According to the former results, integration of solar energy into non-aqueous Li-air battery can effectively reduce the charge overpotential. Hence, we attempt to integrate solar energy into solid-state Li-air battery for constructing a photo-assisted solid-state Li-O_2 battery

Chapter 5 is the general conclusion and proposed suggestions for further improvement on this research work.

Chapter 2 Lowering the charge voltage of Li-O$_2$ battery by photocatalyst coupled with I$^-$/I$_3^-$ redox agent

2.1 Introduction

One of the most important objectives is to lower the charge overpotential and reduce the energy losses during the charge process to achieve a practical Li-O$_2$ battery.[91-95] Practical propulsion batteries are expected to provide "round-trip" energy efficiencies of 90%, but current Li-O$_2$ cells only deliver a low value around 60%-70%, primarily due to the large charge overpotentials.[26; 96-99] Typically, the charge voltage often climbs as high as 4.0 V, which greatly hinders the practical application.[100-104] Therefore，research has mainly focused on finding solutions for the high overpotential issue, including the employment of electrochemical catalyst and redox mediators. Numerous cathode catalyst such as Co$_3$O$_4$ and MnO$_2$ have been reported to be catalytically active for OER process in Li-O$_2$ batteries.[40; 105-108] These transition metal oxides combined with carbon material is proved to drastically improve catalytic activity for Li$_2$O$_2$ decomposition.[66; 109] This OER process involves several steps including the nucleation and growth and requires overcoming a significant reaction barrier, which exhibits as an initiation process for the Li$_2$O$_2$ oxidation. With all these efforts, the charge voltage of 3.5 V is achieved, showing a polarization of ~0.5 V.[101; 110] Another pathway is increasing the solubility of Li$_2$O$_2$, which enable the decomposition of Li$_2$O$_2$ take place in the electrolyte at the electrode surface, thus maximizing the interaction areas. Several research suggested redox mediators as soluble catalyst shows better catalytic activity than the solid counterparts. Redox mediators can readily reach the interior of the air electrode due to the flowing nature even when the products are electrically isolated. In principle, many redox-active molecules show potentials capable for oxidizing solid Li$_2$O$_2$. Accordingly, researchers have reported several types of redox mediators to successfully recharge the Li-O$_2$ battery and reduced charge voltage is achieved, such as TTF, LiI, and TEMPO. With the aid of redox mediators, the charge voltage can be

reduced to ~3.5 V. The charge overpotential of 0.5 V exists which is still high for achieving satisfied energy efficiency and cycle life.

In this regard, we focus on the Li-O_2 battery with the use of a redox mediator. A further reduction on charge voltage of this battery system is highly desired. A very recent work showed that incorporation of a dye-sensitized TiO_2 photoelectrode greatly reduced the charging voltage of Li-O_2 battery, delivering a charging voltage of 2.72 V.[76] We try to introduce a g-C_3N_4 photocatalyst in the air electrode to capture solar energy into the Li-O_2 battery.[111-113] Thus the harvested solar energy can be utilized to compensate the required electric energy. In our proposed battery system, the electrochemical conversion of M^{red}/M^{ox} is gained by photo-driven oxidative reation. In other words, upon charging under illumination, photoexcited electron-hole pairs would generated on the g-C_3N_4 photocatalyst. Due to the high oxidative activity of holes, they would oxidize redox mediator to M^{ox} form.[114-116] In the meanwhile, the photoexcited electrons aid reduction from Li^+ to Li at the anode side. Thus the photovoltage generated between photoexcited holes and electrons could compensate the battery's required charge voltage. The photo-assisted charge strategy combined g-C_3N_4 photocatalyst with redox mediator has been proposed and demonstrated. The charge voltage can be dramatically reduced to 1.9 V and the device stability is also evaluated.

2.2 Experimental and Characterization

2.2.1 Preparation of g-C_3N_4 powder

G-C_3N_4 powder was fabricated according to a calcination approach described in a previous paper.[117] Detailly, melamine powder (Wako, 99%) was heated at 550°C for 3 h in Argon atmosphere with a ramp rate of 2.3°C min^{-1}; the cooling rate was controlled at about 1 °C min^{-1}. The resultant yellow agglomerates were grinded into grain powder in a mortar.

2.2.2 Preparation of g-C$_3$N$_4$ cathode

In order to obtain the g-C$_3$N$_4$/carbon paper composites, the slurry of the melamine and polyvinylidene difluoride (PVDF) in a *N*-methyl pyrrolidone (NMP) was pasted on a carbon paper of 9 mm in diameter, then the composite was heated at 550 °C for 3 h in an Ar atmosphere accompanied with a flow of 37 ml min^{-1} at a ramp rate of 2.3 °C min^{-1}; the cooling rate was maintained at around 1 °C min^{-1}. The mass loading of g-C$_3$N$_4$ active material is 0.16-0.2 mg cm^{-2}.

2.2.3 Preparation of the battery

All the devices were assembled in the glovebox filled with Ar gas. 0.5 M LiClO$_4$ (Wako) and 0.05 M LiI (Wako) dissolved in Tetraglyme (G4, Wako) was employed as the electrolyte. The photoassisted Li-O$_2$ battery was constructed with a Li metal anode, a glass fiber separator (Whatman GF/A) encapsulated with the electrolyte, and a g-C$_3$N$_4$/carbon paper as oxygen electrode and photoelectrode in a coin cell, which had several holes on the top shell. The holes allow the illumination on the photocatalyst. The assembled Li-O$_2$ battery was stored in a sealed glass chamber, which is purged with pure O$_2$ gas for about 3 hours before electrochemical measurements.

2.2.4 Measurements and characterization

X-ray diffraction (XRD) was investigated by employing a Bruker D8 Advanced diffractometer with Cu Kα (λ = 1.5406 Å) radiation. Scanning electron microscopy (SEM) was observed on a Hitachi S4800. ^{1}H nuclear magnetic resonance (NMR) spectrum was recorded on a Bruker 500 MHz spectrometer. The UV-visible absorption spectrum measurements were conducted using a Shimadzu UV3101PC. Galvanostatic discharge/charge test were performed on a Hokuto discharging/charging system. All the electrochemical discharge/charge test were conducted at 25 °C under O$_2$ atmosphere. For the solar-energy irradiation tests, a XEF-501S Xe-lamp (San-ei Electric Co., Japan) was utilized as the light source.

2.3 Results and discussion

2.3.1 Configuration and working mechanism of photoassisted Li-O$_2$ battery

As shown in Fig. 2.1a, the photoassisted rechargeable Li–O$_2$ battery consists of a Li metal anode, an electrolyte combined with the LiI redox mediator and C$_3$N$_4$ grown on carbon paper as an air electrode and a photoelectrode simultaneously. It is worth noting that g-C$_3$N$_4$ serves not only as a photocatalyst, but also as an oxygen reduction reaction (ORR) electrocatalyst. In the practical operation, the battery assembly was performed in a 2032 coin cell with holes on the top shell allowing the direct irradiation on photocatalyst, as exhibited in Fig. 2.1b. For the photo-electric conversion tests, a sunlight simulated machine was employed as the light source.
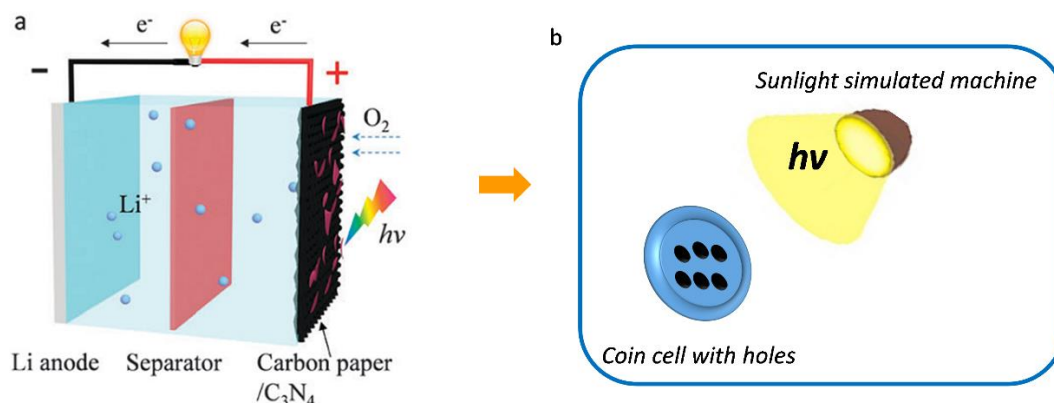
Fig. 2. 1 a) The schematic illustration for photoassisted Li-O$_2$ battery b) The schematic for experimental operation of photo-electric conversion

In the photoassisted battery, the discharge process is same to that of a conventional Li-O$_2$ battery with the formation of Li$_2$O$_2$ (Fig. 2.2a). On charging under illumination, the I$^-$ ions are initially oxidized to I$_3^-$ ions by photoexcited holes derived from the photocatalyst (Reaction 1, Fig. 1.9a),[118] and subsequently I$_3^-$ ions diffuse to the surface of oxygen electrode and chemically decompose Li$_2$O$_2$ to O$_2$ and reduced back to I$^-$ ions, thus complete a full redox cycle (Reaction 2, Fig. 2.2a). In the meanwhile, the

photoexcited electrons transfer to the anode side via the external circuit, and reduces Li^+ ions to Li metal (Reaction 3, Fig. 2.2a). Therefore, the charging voltage of a Li–O_2 battery is compensated by the photovoltage on the g-C_3N_4 photoelectrode. As presented in Fig. 2.2.b, the photoassisted charging voltage corresponds to the energy difference between the redox potential of Li^+/Li and the conduction band potential (CB) of the photocatalyst. A proper photocatalyst for the photoassisted rechargeable battery has to satisfy two critical conditions: the CB potential should be lower than the O_2/Li_2O_2 redx potential (that is, 2.96 V) and the valance band (VB) potential should be higher than the I^-/I_3^- couple potential to drive the oxidative reaction of I^- ions to I_3^- ions based on Fig. 2.2b. As a metal-free photocatalyst, g-C_3N_4 exhibits an conduction band potential of 1.7 V, much lower than that of TiO_2 photocatalyst (2.6 V). By using the g-C_3N_4 photocatalyst, the photoassisted charge voltage of the Li–O_2 battery can be reduced to 1.7 V in theoretical.[119-122] On the other hand, g-C_3N_4 has been recently demonstrated to be an efficient electrocatalyst for ORR and oxygen evolution reaction (OER).[123; 124]
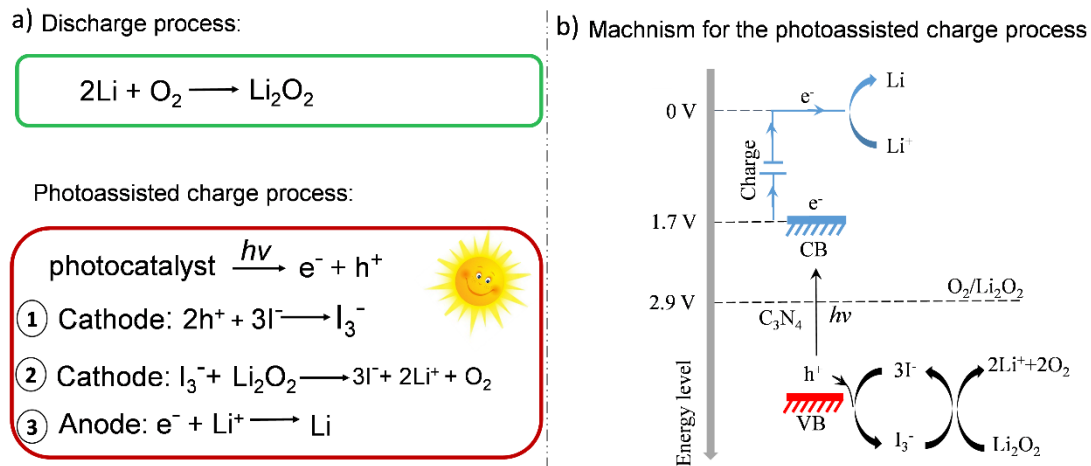
Fig. 2.2 a) The reaction mechanism for the photoassisted Li-O_2 battery b) The energy diagram for the photoassisted charging process

The crystalline structure of g-C_3N_4 is analysed by X-ray diffraction (XRD) pattern (Fig. 2.3a) in which two typical signals are observed, including the peak at 27.5° (2θ), assigning to graphite-like layers of 0.326 nm, and the peak at 13.3° (0.713 nm) arising

from repeated tri-*s*-triazine units.[27] The bandgap of the condensed graphic carbon nitride is estimated to be 2.7 eV as determined by ultraviolet-visible (UV-Vis) spectrum (Fig. 2.3b), showing an intrinsic absorption in the blue region of the visible light. To prove that I^- ions can be oxidized to I_3^- ions by photoexcited holes from g-C_3N_4, a solution composed of 0.05 M I^- ions with g-C_3N_4 powders is illuminated for 1 h and then characterized by the UV-Vis absorption spectrum. Fig. 2.3c exhibits two peaks at 288 and 350 nm featuring the I_3^- ions, which suggests that I^- ions can be oxidized by the photoexcited holes from g-C_3N_4. Besides, a porous air electrode framework will benefit for the rapid transport of I^-/I_3^- ions and prohibit clogging by the Li_2O_2 particles. Therefore, coupled with LiI redox mediator, g-C_3N_4 grown on porous carbon fibre paper is simultaneously used as an oxygen electrode and a photoelectrode.
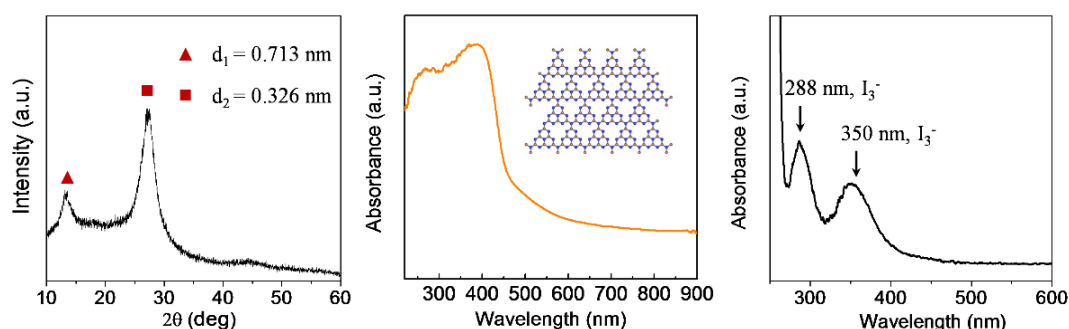
Fig. 2.3 (a) XRD pattern and (b) UV-Vis absorption spectrum of the g-C_3N_4 photocatalyst. (c) UV-Vis absorption spectrum of 0.05 M I^- ions solution with g-C_3N_4 powders after 1 h irradiation.

2.3.2 Reduced charge voltage of photoassisted Li-O_2 battery

Fig. 2.4 shows the comparison of charging/discharging profiles of a normal Li–O_2 battery without the I^- ion redox mediator, a Li–O_2 battery with the I^- ion redox couple and the photoassisted Li–O_2 battery tested at 0.01 mA cm^{-2}. The normal Li–O_2 battery without using I^- ion redox mediator shows a typically high charging voltage (ca. 4.1 V), by contrast, a reduced charging voltage (ca. 3.55 V) could be attained with the aid of

the soluble I^- ion redox mediator. After integration of the g-C_3N_4 photocatalyst, the charging voltage decreases dramatically to 1.9 V, which is identical to the theoretical prediction of energy difference (ca. 1.7 V) between the CB of g-C_3N_4 and Li^+/Li couple potential. The results are consistent well with the theoretical prediction, showing the lowest charging voltage for a Li–O_2 batteries so far. It is worth noted that the charging voltage is much lower than the discharging voltage (2.73 V, as shown in Fig. 2.4), resulting in an electrical energy efficiency of 142%. It is clear that such a high energy efficiency is owing to the illumination.
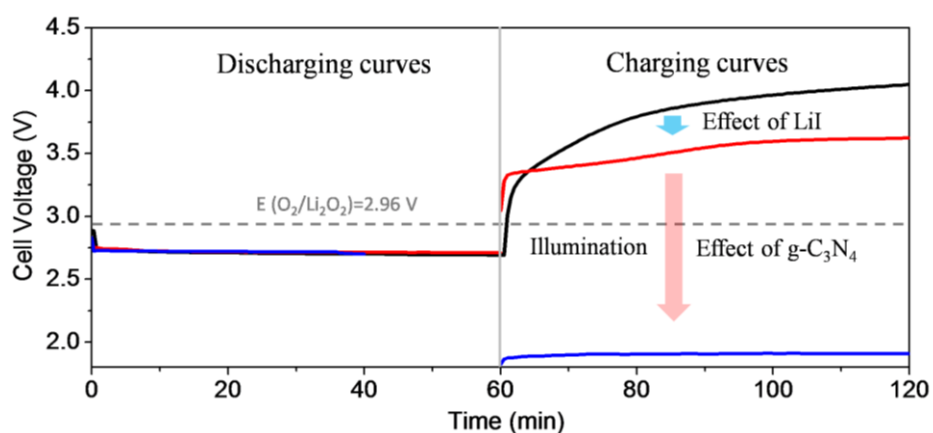
Fig. 2.4 The charging/discharging curves of a normal Li–O_2 battery without the I^- ion redox mediator (black line), a Li–O_2 battery with the I^- ion redox couple (blue line) and the photoassisted Li–O_2 battery (red line).

Besides, the stability of G4 solvent under long-term irradiation was also investigated to avoid any confusion in the proposed battery system. No detectable change in the ^1H nuclear magnetic resonance (NMR) spectroscopy of G4 electrolyte can be observed after 5 h illumination, as shown in Fig. 2.5, suggesting favorable stability of the electrolyte (G4) under long-term illumination. For the proposed photoassisted rechargeable battery, the charging process are equivalent to the oxidative process of I^- to I_3^- ions, which could decompose Li_2O_2 through a chemical reaction.
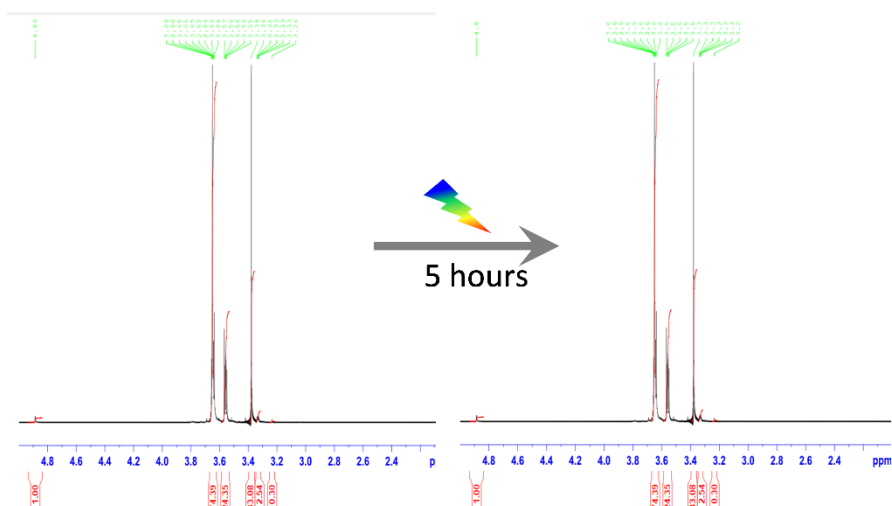
Fig. 2.5 ^{1}H NMR spectra of 1M LiClO$_4$ and 0.05 M LiI dissolved in G4 electrolyte (a) before and (b) after 5 h irradiation.

To further demonstrate this reaction, XRD and scanning electron microscopy (SEM) were used to detect the discharge product after 8 h discharge at 0.1 mA cm^{-2} and a charge product after 4 h charge at 0.2 mA cm^{-2}, resulting in an equivalent discharge-charge capacity. The results demonstrate that the discharge product is Li$_2$O$_2$, while the peaks corresponding to Li$_2$O$_2$ disappeared after the subsequently photoassisted charge (Fig. 2.6), implying that Li$_2$O$_2$ has been completely removed by the I$_3^-$ ions at the end of charge.
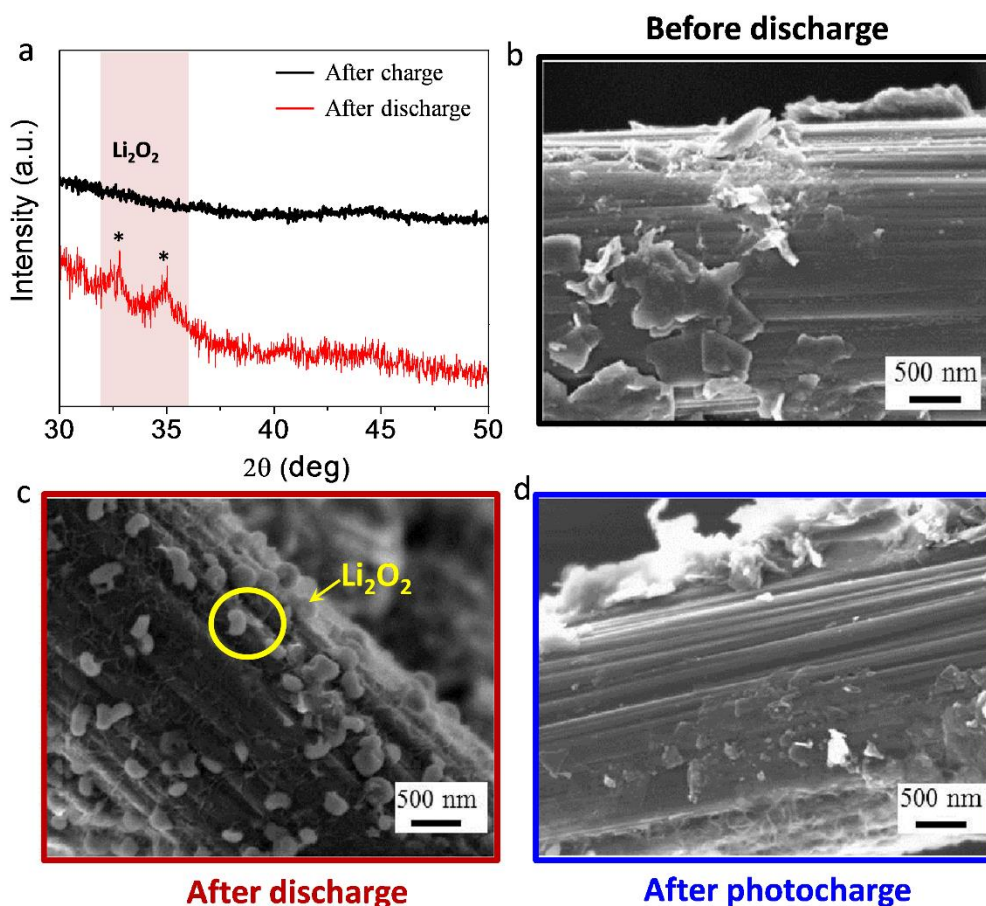
Fig. 2.6 (a) XRD patterns of the discharge and charge products. SEM images of cathodes observed at pristine (b), after discharge (c) and after photoassisted charge processes (d), scale bar is 500 nm.

2.3.3 Rate capability and cycling stability

The charging and discharging curves at different current densities are evaluated as shown in Fig. 2.7a, b. It is noticeable that the polarization degree does not dramatically increase. The photoassisted charging voltage presents as 2.23 V, even at a current of 0.03 mA cm^{-2}. To investigate the stability of this device, we studied the photoassisted charging cyclability (Fig. 2.7c, d). After 50 repeated cycles (1 h photoassisted charging and then 1 h discharging), the battery can still maintain a charging voltage around 2.2 V, indicating the good stability of g-C$_3$N$_4$ photoelectrode.
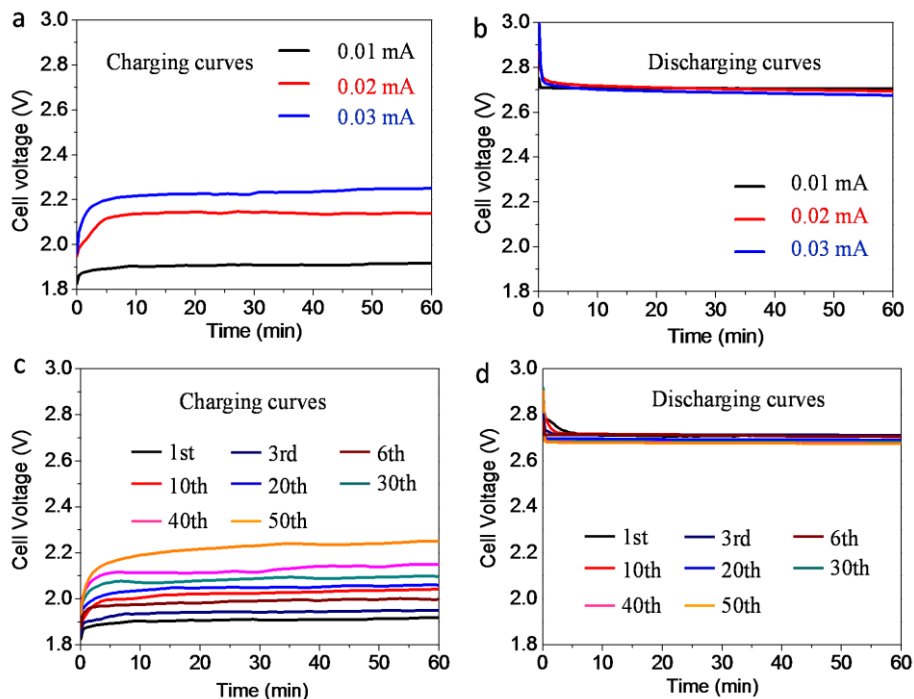
Fig. 2.7 (a) The charging profiles and (b) the discharging profiles of the photoassisted Li-O$_2$ battery at various current densities. (c) The charging curves and (d) the discharging curves of the photoassisted Li-O$_2$ battery at 0.01 mA cm^{-2} for 50 cycles.

2.4 Conclusions

It is noted that the g-C$_3$N$_4$ plays an important role on the effective realization of the photoassisted rechargeable Li-O$_2$ battery. Firstly, the CB potential of g-C$_3$N$_4$ photocatalyst is inherently lower than most of photocatalysts such as TiO$_2$, ZnS, CuO, and Ta$_3$N$_5$, offering an ultralow photoassisted charging voltage in theoretical. Moreover, g-C$_3$N$_4$ with a suitable bandgap (~2.7 eV) can directly absorb visible light without the further modification with unstable organic dyes. Accordingly, compared with the dye-sensitized TiO$_2$ photoelectrode, it showed improved cycling performance.[125; 126] More importantly, the g-C$_3$N$_4$ can also serve as ORR electrocatalyst for Li-O$_2$ battery and thus simplify the device as two-electrode system, which facilitates the practical application.

By introducing a g-C$_3$N$_4$ photocatalyst into Li-O$_2$ battery, we demonstrate that the charging voltage can be effectively reduced to 1.9 V, the lowest for a Li-O$_2$ battery up

to date. During the photoassisted charging process, the photoexited electrons from g-C_3N_4 transfer to the anode side and reduce Li^+ to Li and thus the photovoltage on g-C_3N_4 is utilized to compensate the battery's required charging voltage. Meanwhile, I^- ions redox mediator are oxidized to I_3^- by the photogenerated holes and then, in turn, chemically oxidize the Li_2O_2 particles; in this process, I_3^- is reduced back to the initial I^-. The photoassisted charging strategy effectively addresses the high overpotential issue facing the $Li-O_2$ battery. It is worth pointing out that the charging voltage is even lower than the discharging voltage ($\sim$2.7 V), resulting in a 142% electrical energy efficiency. The concept of "energy saving" can be extended to other battery systems and thus contributes to the progress of advanced energy storage techniques.

Chapter 3 Lowering the charge voltage of Li-O$_2$ battery via an unmidiated photoelectrochemical method

3.1 Introduction

Redox mediators play a critical role in reducing the high charge overpotential issue, serving as an electron–hole transfer agent between the solid electrode and solid Li$_2$O$_2$ particles.[83; 127-134] As discussed above, numerous redox mediators have been successfully applied. Lim et al. introduced LiI as a redox mediator and successfully reduced the charge potential to 3.2 V by combining with the hierarchically carbon nanotube cathode.[75] Yu et al. demonstrated a low photoassisted charge voltage of 2.72 V for Li–O$_2$ batteries by employing I$^-$/I$_3^-$ redox mediator integrated with a TiO$_2$ photoelectrode.[76] However, severe side reaction and shuttle effect related to redox mediator has been demonstrated. During the charge process, LiI dissolved in elelctrolyte can easily be electrochemical oxidized to form I$_3^-$, and can then diffuse to lithium anode where they are reduce to LiI. The LiI is then partially dissolved in electrolyte and I$^-$ ions are oxidized to I$_3^-$ again. The above process take place repeatedly showing as the "shuttle effect" and has been proved by Zhang et.al.[135] Additionally, Kwak et al. demonstrated the side reaction of LiOH formation when a high concentration of LiI is used.[136]

In this case, we propose, removing the redox mediator, an unmediated oxidization reaction of solid Li$_2$O$_2$ by photoexcited holes derived from the photoelectrode. As a result, an ultralow photoassisted charge voltage of 1.96 V and a typical discharge voltage of 2.74 V are attained. By this unmediated photooxidation methode, the cycling performance of photoassisted Li-O$_2$ battery is enhanced.

3.2 Experimental and characterization

3.2.1 Synthesis of g-C$_3$N$_4$-CP electrode

Graphitic-carbon nitride, hereafter recorded as g-C$_3$N$_4$, is prepared from a simple precursor via a series of thermal polycondensation reactions without any metal involvement. The g-C$_3$N$_4$-CP was fabricated as follows: the guanidine hydrochloride (GundCl) precursor and polyvinylidene fluoride (PVDF) powder were mixed with a mass ratio of 95:5, dissolving in N-methyl pyrrolidine (NMP) solvent, and then grinded for 30 min to blend homogeneously.[137; 138] Then the carbon fiber paper (dia. 7 mm) was dipped into the obtained solution and pasted with the mix slurry. The g-C$_3$N$_4$-CP was finally attained after calcination at 550 °C for 3h under Ar atmosphere with a heating rate of 2.3 °C min^{-1}; The cooling rate was controlled at around 1°C min^{-1}. The loading mass of g-C$_3$N$_4$ on g-C$_3$N$_4$/carbon paper cathode is about 0.4 mg cm^{-2}. The weight ratio between carbon fiber paper (~2.4 mg) and g-C$_3$N$_4$ (0.4 mg) is about 6 : 1.

3.2.2 The photoassisted Li-O$_2$ Battery assemble:

All the battery assembly was carried out in an Ar gas filled glovebox using 2023 coin cell with several holes on top, which enable the direct illumination on the photoelectrode. The electrolyte was comprised of 1 M Lithium bis(trifluoromethanesulfonyl)imide (LiTFSI, Sigma) dissolved in Tetraglyme solvent (G4, WAKO). The photoassisted rechargeable Li-O$_2$ battery was consisted with a Li metal as anode, a glass fiber as separator filled with electrolyte and a g-C$_3$N$_4$-CP as oxygen electrode also photoelectrode. The assembled battery was stored in a glass jar with a volume of 650 mL, and flow with O$_2$ before the electrochemical investigation. The light source used for the solar energy conversion is a XEF-501S Xe-lamp (San-ei Electric Co., Japan). The charging/discharging tests for the all devices were conducted at various current densities by using a Hokuto electrochemical system.

3.3.3 Measurements and characterization

X-ray diffraction (XRD) analysis was performed by a Bruker D8 X-ray diffractometer using Cu Kα (λ=1.54 Å) radiation. The chemical constitution of g-C$_3$N$_4$-CP was featured by X-ray photoelectron spectroscopy (XPS, Thermo Escalab 250, with a monochromatic Al K$_α$ X-ray source). Scanning electronic microscope (SEM) was performed on a Hitachi S4800. Galvanostatic discharge/charge was carried out on a Hokuto discharging/charging machine. FTIR was attained on a JASCO instrument of FT/IR-6200 from 1300 to 900 cm^{-1} and the resolution is 2 cm^{-1}.

3.3 Results and discussion

3.3.1 An unmediated photoelectrochemical oxidation methode

We studied the shuttle effect caused by redox mediators, with LiI as an example, on the metallic Li anode by using Fourier transform infrared (FTIR) measurements. A cell was constructed with a Li metal anode, a LiTFSI in G4 electrolyte with 0.1 M LiI additive, and a g-C$_3$N$_4$ cathode/photoelectrode. Under illumination, the I$^-$ ions in electrolyte can be oxidized to I$_3^-$ ions by photoexcited holes originated from g-C$_3$N$_4$, then I$_3^-$ ions transfer onto the Li anode side and thereby form LiI layer. Fig. 3.1a shows the FTIR measurements for the surface resultants of Li anode after irradiation. After 6h illumination, the peaks at around 1100 cm^{-1} corresponding to LiI is identified in the spectra, proving the shuttle reaction between I$_3^-$ ions and Li anode. The LiI formed on the surface of the Li anode is further evidenced by scanning electron microscopy (SEM) (Fig. 3.1b,c). After illumination for 6h, the surface of Li anode obviously roughened due to the accumulation of LiI grains. This shuttle reaction can lead to the decrease of the active utilization of I$_3^-$ ions and thus result in detrimental influence on the Li anode.
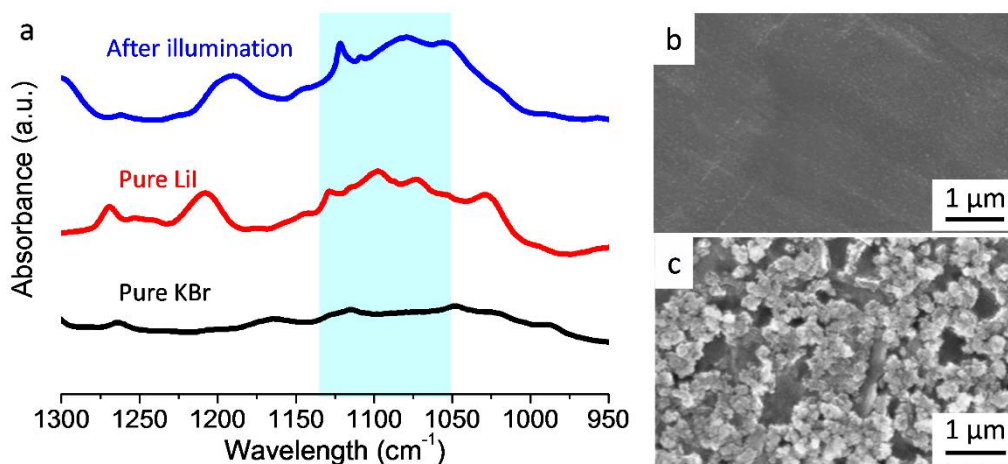
Fig. 3.1 (a) The FTIR spectra of the surface of Li anode after irradiation for 6 h in G4 with LiI, pure LiI and the reference KBr. SEM images of the Li anode (b) before and (c) after irradiation for 6 h in G4 with LiI

Thereby, we proposed an unmediated photoelectrochemical oxidation strategy to reduce the charge overpotential of Li-O_2 batteries. Owing to absence of redox mediator, different from the photoassisted Li-O_2 battery reported, our battery shows a more operational flexibility configuration: a metallic Li anode, a separator filled with LiTFSI/G4-based electrolyte and g-C_3N_4-CP simultaneously served as an oxygen electrode and a photoelectrode. During the discharge, O_2 is reduced and combined with Li^+, producing insoluble Li_2O_2 products that deposite evenly as a thin layer on the surface of g-C_3N_4 coating. The working mechanism of the photoassisted charge process is schematically illustrated in Fig. 3.2. Fig. 3.2a shows the illustration of a g-C_3N_4-CP interface where the g-C_3N_4 photocatalyst, is excited upon absorption of photons to generate hole-electron pairs, with holes oxidizing Li_2O_2 to O_2 and electrons injecting into carbon paper, and aiding the reduction of Li^+ to Li metal. At the cathode side, photogenerated holes could directly oxidize Li_2O_2 to produce Li^+ and O_2 gas due to the driving force between valence band (VB) potential (4.4 V (all potentials are referenced to Li^+/Li couple)) g-C_3N_4 and Li_2O_2/O_2 redox potential.[139-142] During the charge process, the photovoltage on g-C_3N_4 photocatalyst is utilized to compensate the battery´s charge voltage. The theoretical photoassisted charge voltage is determined by the energy difference between the Li/Li^+ redox potential and conduction band (CB) position of g-C_3N_4 photocatalyst (that is 1.7 V) (Fig. 3.2b).
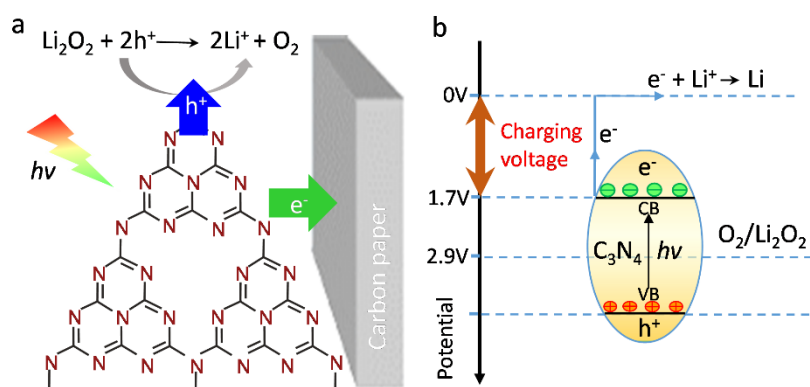
Fig. 3. 2 (a) Illustration of a g-C$_3$N$_4$-CP electrode interface. (b) The theoretical potential diagram of the photoassisted charge voltage, equivalent to the energy difference between the redox potential of Li$^+$/Li and CB level of g-C$_3$N$_4$ (ca. 1.7 V).

The photoassisted Li-O$_2$ battery contained g-C$_3$N$_4$-CP cathode was assembled as described in the Experimental section. The charge/discharge capability of the battery were studied, with and without irradiation, to provide a back-to-back comparison at 0.01 mA cm^{-2}; the results are presented in Fig. 3.3. The dashed line in the middle represents the theoretical charge/discharge voltage for a Li-O$_2$ battery. Without illumination, the Li-O$_2$ battery exhibits an initial voltage of 3.61 V based on the potential at the half-charge capacity point, which is similar to previously reported results employed g-C$_3$N$_4$ as an OER catalyst.[32] In sharp contrast, upon charging under illumination, the charge voltage drastically decreased to 1.96 V that is even lower than the Li$_2$O$_2$/O$_2$ redox potential ($\sim$ 2.96 V),[143] thus resulting in a 'negative' charge overpotential. The obtained charge voltage is well identical to the theoretical energy difference between the CB level of g-C$_3$N$_4$ and Li$^+$/Li redox potential (1.7 V). By employing g-C$_3$N$_4$-CP as an ORR catalyst, the battery shows a standard discharge voltage of 2.74 V. The great voltage gain could contribute to a relatively high electrical energy efficiency (ca. 140%).
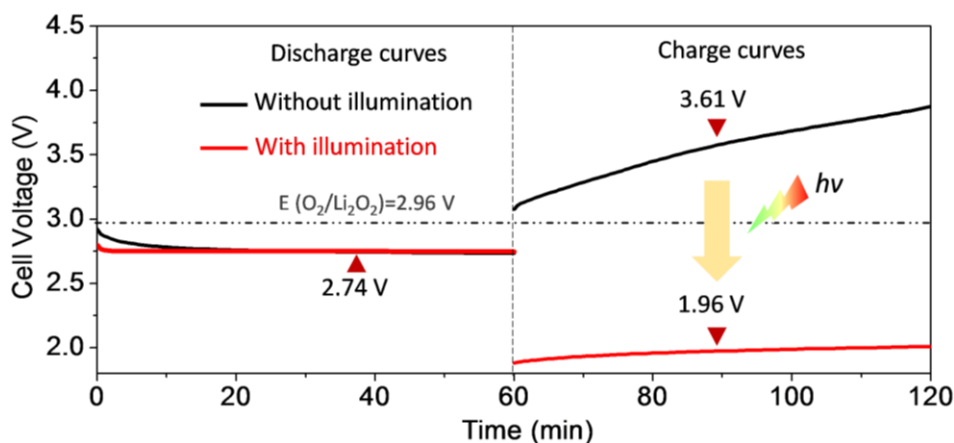
Fig. 3.3 The charge/discharge profiles of Li-O$_2$ battery with (red line) and without illumination (black line).

To better understand the photoassisted charge process, we performed ex situ analysis on the cathode at different states-of-discharge/charge. At specified points along the discharge/charge test (Fig. 3.4a) we disassembled the cells, fetched the cathode from those cells, washed away the contained electrolyte, then visualized the Li$_2$O$_2$ discharge products by scanning electron microscopy (SEM); we also collected XRD patterns of samples to identify the chemical composition of the discharge products. The photoassisted rechargeable Li-O$_2$ battery was firstly discharged for 6 h, and subsequently charged for 6 h under irradiation at the current of 0.04 mA cm^{-2}. The capacity of 600 mAh/g$_{g-C3N4}$ is considered as a relatively deep discharge. The discharge voltage and photoassisted charge voltage present at around 2.69 and 2.42 V, respectively. Of note, the battery shows a modest increase in charge voltage because the charge transfer between Li$_2$O$_2$ products and the g-C$_3$N$_4$ photoelectrode surface becomes increasingly hard with an increase in rate. After discharge for 3h, upon nucleation, small islands of Li$_2$O$_2$ particles are distributed uniformly on the surface of g-C$_3$N$_4$ layer. By the end of 6 h discharge, the g-C$_3$N$_4$-CP electrode from the battery shows even larger Li$_2$O$_2$ particles deposition, up to about 200 nm.[144-147]

After photoassisted charge for 3h, the Li$_2$O$_2$ particles turn into relatively fine again, demonstrating that the photogenerated holes generated upon irradiation do, indeed, go on to oxidize Li$_2$O$_2$ particles. By the end of photoassisted charge process, the SEM

34

image validates that Li_2O_2 particles are completely decomposed, suggesting the reversiblility of formation and decomposition of Li_2O_2 products. XRD analysis was conducted to further probe the discharge and charge products with a cutoff time of 6 h at 0.1 mA cm^{-2}. After discharge, the typical diffraction peaks assigned to Li_2O_2 can be clearly observed, then disappeared after the photoassisted charge process as shown in Fig. 3.4b, indicating that the Li_2O_2 particles could be completely scavenged by the photoassisted charge strategy that agrees well with the SEM images. These results verify that the Li_2O_2 can be efficiently decomposed by the photoexcited holes derived from photoelectrode upon irradiation.
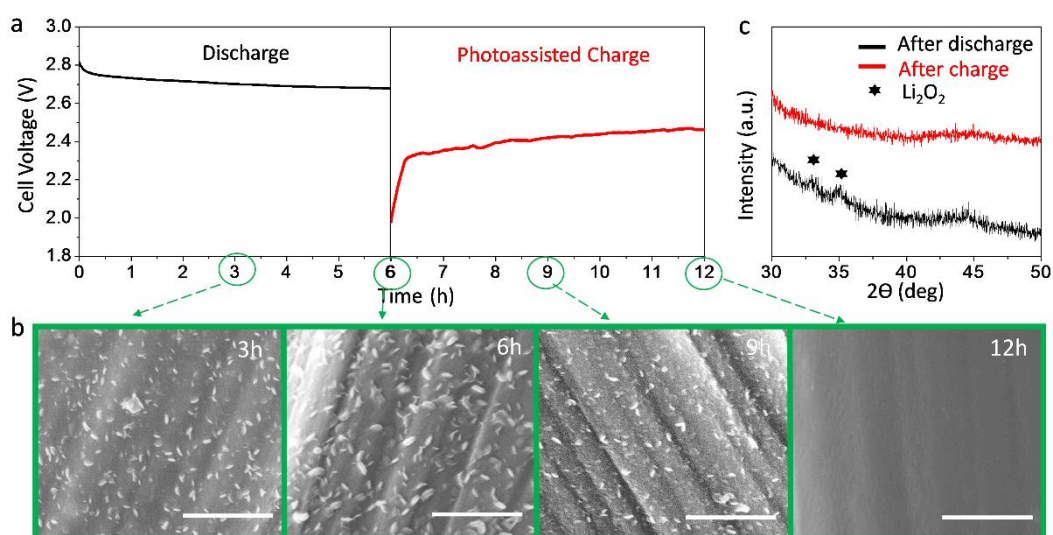
Fig. 3.4 (a) The charge/discharge curves of photoassisted $Li-O_2$ battery at 0.04 mA cm^{-2}. (b) SEM images of discharge products at different stages during charge/discharge test. Scale bars, 1 μm. (c) XRD patterns of the discharge/charge products with a cut-off time of 6 h at 0.1 mA cm^{-2}.

3.3.2 Rate capability and cycling stability

The cycling performance of the photoassisted $Li-O_2$ battery was evaluated by the galvanostatic charge/discharge test at 0.01 mA cm^{-2}. The entire 70 cycles voltage profiles as well as the magnified 1st and 70 th cycle profiles are as presented in the Fig. 3.5a,b. The black and red lines in the figure 3.5 represent, respectively, the discharge and photoassisted charge voltage profiles. Even after irradiation for 70 h over 70

repeated photoassisted charge and discharge circles, the charge voltage is still recorded at about 2.35 V. On the other hand, discharge voltage only declines by ~0.06 V after the 70 repeated cycles, implying that structure of g-C_3N_4-CP electrode is relatively stable even irradiated for a long time. The discharge and photoassisted charge curves of the cell at different current densities of 0.01, 0.03 and 0.05 mA cm^{-2} are shown in Fig. 3.5c. Although it is noticeable that the polarization trends during charge process increased slightly as the increase of current densities, the voltage plateau can still maintain at 2.4 V even at 0.05 mA cm^{-2}. We also investigated the cycling ability of the batteries at high current densities of 0.05 mA cm^{-2}. Upon 10 cycles, the battery can still record a charge voltage of 2.45 V (Fig. 3.5d).
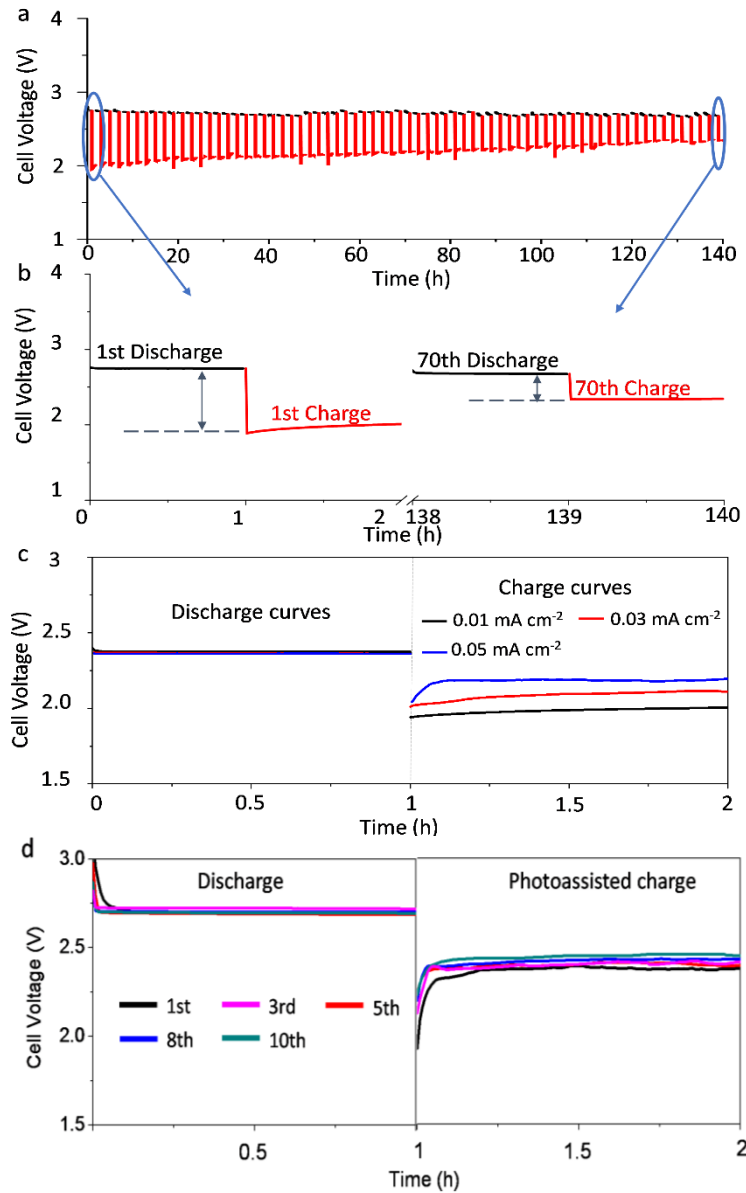
Fig. 3.5 (a,b) The photoassisted charge and discharge profiles at the current density of 0.01 mA cm^{-2}. (c) the discharge and photoassisted charge profiles at various current densities. (d) The discharge and photoassisted charge curves at 0.05 mA cm^{-2} for 10 cycles.

3.4 Conclusions

Applying the g-C$_3$N$_4$ coating CP structure as both cathode and photoelectrode offers direct contact between Li$_2$O$_2$ particles and the g-C$_3$N$_4$ photocatalyst, meanwhile promotes photoexcited carriers transportation. Benefit from the proper design, the photogenerated holes from the photocatalyst can directly react with the Li$_2$O$_2$ particles without the aid of redox mediators. We successfully address the severe charge overvoltage challenge of Li-O$_2$ battery via the unmediated photo-oxidative approach. Besides, photocharging batteries reported to date have generally coupled photocatalyst with liquid redox mediators for solar energy utilization.[148-151] However, due to the photo/thermal instability of liquid organic electrolyte under irradiation, all-solid-state batteries represent a promising avenue for future solar energy conversion/storage. From a broader perspective, this unmediated photo-oxidative approach lay a foundation for the further development of photocharging solid-state batteries.

Chapter 4 Improving the electric energy efficiency of solid-state Li-O$_2$ battery

4.1 Introduction

With the increasing requirements imposed by electric vehicle (EV), the energy storage devices possessing high capacity and enhanced safety are highly anticipated. Li-O$_2$ battery is considered as a competitive candidate among various energy storage devices,[152-155] such as Li-ion battery,[156] sodium-ion battery,[157] supercapacitors.[158] However, they entail the risks of fire or explosion caused by the use of combustible organic electrolytes caused by the use of combustible organic electrolytes. [159; 160] From the perspective of safety, the solid-state Li-O$_2$ battery has been demonstrated as a viable solution for the power source of EV.[161] While, some fundamental issues in solid-state Li-O$_2$ battery are still hang in doubt, especially the large interfacial resistance between electrolyte and electrodes and thereby leading to the significant charge transport barrier during charging process, high charge overpotential and low energy efficiency. This has becomes the bottleneck for the further advance of solid-state Li-O$_2$ batteries.

Therefore, numerous research efforts are being devoted to reduce the high charge voltage derived from severe interfacial behavior, such as the adoption of noble metal as electrocatalysts (Ru,[162] Pd,[163] Au[164]) and the design of efficient air electorde interface.[165-169] Nevertheless, these methods usually suffer from some undesired parasitic reactions (such as shuttle effect, electrolyte decomposition) and high cost. Despite these attempts, the high charge voltage (> 4.0 V) of solid-state Li-O$_2$ battery is still unfavorable.

In this study, we therefore focus on improving the electric energy efficiency of solid-state Li-O$_2$ batteries caused by large interfacial resistance. Based on the previous studies, it is suggested that the introduction of photocatalysis into aprotic Li-O$_2$ battery can effectively alleviate the overpotential issue since the captured solar energy can be used to reduce electric energy input.[170-172] Thanks to its better photo/thermal stability, the

integration of solar energy into solid-state Li-O$_2$ battery is an effective pathway to address the charge overpotential issue facing in solid-state Li-O$_2$ battery. On the other hand, integrating solar energy with solid-state Li-O$_2$ battery provides an inspirational avenue for efficient solar energy utilization.[173; 174] The solid-state Li-ion O$_2$ battery exhibits an ultralow charge voltage (2.08 V) and high energy efficiency (113%, based on output electric energy/input electric energy) under irradiation. Consequently, the conversion and storage of solar energy are simultaneously realized through this device, which also displays promising implementation in flexible electronic devices.

4.2 Experimental and characterization

4.2.1 Preparation of cathode

Synthesis of ZnS@CNT composite: The ZnS@CNT composite is prepared based on a modified method reported in previous paper[175]. In detail, CNTs (sigma aldrich) are homogeneously dispersed in 40 ml of ethylene glycol solution (EG, >99.5% Wako Chemicals) using ultrasonication. Next, 0.25 mmol of zinc acetate (Wako Chemicals, 99%) and 0.25 mmol of thiourea (Wako Chemicals, 99%) were added into the above solution and stir for 1 h to blend uniformly. The resultant solution is subsequently transferred to a 50 ml autoclave and kept at 180℃ for 6 h. After naturally cooling to room temperature, the obtained samples are collected by centrifugation, rinsed with deionized water and ethanol repeatedly to remove impurities. Finally, the sample is dried in air for over 12 h at 60 ℃.

The cathode is fabricated as follow: the obtained ZnS@CNT composite and polyvinylidene fluoride (PVDF) powder are mixed with a mass ratio of 9:1, and then dissolved in N-methyl pyrrolidine (NMP) solvent to form an uniform slurry. The slurry is coated on a carbon fiber paper of 7 mm in dia. Before using, the cathodes are dried in vacuum oven at 80 °C for 12 h.

4.2.2 Preparation of anode

To fabricate the lithiated Silicon (Li_xSi) electrode, a half cell consisted of Li metal anode and Si electrode cathode is assembled wherein the Li^+ ions are electrochemically insert into Si material.[176] Firstly, the Si electrode is produced by blending the commercial Si powder (crystalline, ~ 50 nm, Alfa Aesar), super P carbon and polyacrylic acid binder with a ratio of 70 : 20 : 10 wt%. The resultant slurry is then pasted onto a Cu foil. The mass loading of Si electrodes is about 0.6 mg cm^{-2}. Prior to the battery assembly, the Si electrodes are vacuum dried in an oven at 80°C overnight. The electrolyte is prepared by dissolving 1 M Lithium bis(trifluoromethanesulfonyl)imide (LiTFSI, sigma Aldrich, 99.95%) in tetraglyme (G4, sigma aldrich, 99%) containing 5 wt% Fluoroethylene carbonate (FEC). Herein, FEC is applied as an additive to contribute the formation of solid electrolyte interphase (SEI) film on Si electrode surface. In the galvanostatic test, the Si electrode is lithiated through discharging Li ion half battery to 0.01 V at 200 mA g^{-1}. Figure S1 shows the initial discharge/charge curves at a current density of 200 mA g^{-1}, which corresponds to a good coulombic efficiency (84%). We disassembled this half cell, retrieved and rinsed the Li_xSi electrode, which was then employed as anode for the solid-state Li-ion O_2 battery.

4.2.3 Battery assembly

All battery assembly are performed in the glovebox flow with Ar gas. The proposed solid Li-ion O_2 battery is constructed in a 2032 coin cell which has 7 holes on top, permitting the irradiation onto the ZnS photoelectrode. In this work, the solid electrolyte is comprised of 5 mol% LiTFSI dissolved in succinonitrile (SCN) which features as plastic-crystal form with a melting point of 65°C. The as-prepared

electrolyte presents as liquid state above 65 ℃ while becomes solid state below 65 ℃. Thereby, the LiTFSI/SCN electrolyte is heated to 70 ℃ and becomes liquid state before using. The proposed photoassisted solid-state battery is assembled with a Li_xSi as anode, a separator (glass fiber) filled with electrolyte and a ZnS@CNT composite as air electrode and photoelectrode. The as-assembled Li-ion O_2 battery is put in a glass jar flowing with O_2 gas for 2 h before electrochemical measurements.

As to flexible solid-state battery, carbon textile instead of carbon paper, is chosen as the current collector. The fabrication of flexible battery is the same as described previously. After battery assembly, the flexible cell is attached on a cylindrical glass bottle to be fixed under bendable state.

4.2.4 Characterizations:

For the photo-electric conversion tests, a sunlight simulated machine employed for the irradiation is a XEF-501S Xe-lamp (Sanei Electric Co., Japan). Galvanostatic electrochemical tests were conducted on a Hokuto discharging/charging machine. The X-ray diffraction (XRD) measurements were conducted on a Bruker D8 diffractometer with Cu Ka (λ=1.54 Å) radiation. The chemical state of ZnS@CNT composites is investigated by using X-ray photoelectron spectroscopy (XPS, PHI 5000 VersaProbe), Scanning electron microscopy (SEM) images are observed via a Hitachi SU-8010. The thermogravimetric analysis (TGA) results are attained on BRUKER TG-DTA 2010SA-G4H. Transmission electron microscopy (TEM) images are visualized by a JEOL JEM-200CX. The Raman spectra measurement is performed on a JASCO microscope spectrometer (NRS-1000DT).

4.3 Results and Discussion

A proper photocatalyst is the prerequisite to realize the photo-driven charging strategy, which is required to fulfill two conditions: 1) The conduction band (CB) level of photocatalyst should lie lower than O_2/Li_2O_2 redox potential for compatibility with Li_2O_2 formation/decomposition (2.96 V vs Li/Li$^+$, all potentials described in this work are referred to Li/Li$^+$). 2) The valence band (VB) level should lie higher than the

O_2/Li_2O_2 couple potential to drive the chemical reaction between holes and Li_2O_2 products. Owing to the specific band positions (CB: 2.0 V, VB: 5.6 V), ZnS is chosen as an ideal photocatalyst to realize the solar-driven oxidation of Li_2O_2 and further reduce the high overvoltage in solid-state Li-O$_2$ batteries.[177; 178]Therefore, zinc sulfide@carbon nanotube (ZnS@CNT) composite serves not only as an oxygen electrode but also a photoelectrode in the battery. Before constructing the photoassisted solid battery, the electrochemical performance of ZnS was investigated to avoid any misunderstand in the photoassisted charge reactions. According to the discharge/charge profiles (as shown in Figure S1), it is demonstrated that ZnS presents negligible electrochemical activity, which can hardly contribute electrochemical capacity in this study.

On the other hand, lithium metal is attracted intense attention as anode since the guarantee for high energy density. However, it is problematic for practical application, such as the inferior Coulombic efficiency and Li dendrite formation during cycling. Fortunately, Silicon (Si) has emerged as a promising candidate for replacing Li anode because of its large theoretical capacity (4200 mAh g^{-1}). In this regard, replacing Li metal with Li$_x$Si anode would be a potential way for energy-density improvement as well as safety modification.[179; 180] Accordingly, owing to the enhanced capability of Si anode prior to lithium anode, the photoassisted solid-state battery is constructed with Li$_x$Si, which is attained by the electrochemical lithiation of commercial silicon material. The Li$_x$Si electorde delivers a favorable capacity of 3350 mAh g^{-1} that is comparable to Li anode (3860 mAh g^{-1}) (Figure S2).

As designed, the proposed photoassisted solid-state battery is assembled with a Li$_x$Si anode, a plastic-crystalline solid electrolyte (LiTFSI/SCN) and a ZnS@CNT cathode, as illustrated in Fig. 4.1a. By utilizing ZnS photocatalyst, the solid-state Li-ion O$_2$ battery could be charged at an ultralow voltage of 2.08 V under irradiation. Such a voltage is even lower than the theoretical value (~2.86 V) with the Li$_x$Si/Si couple as counter and reference electrodes (seen in Figure 4.1b). The low charge voltage directly elevates electric energy efficiency to 113%. Compared with normal solid Li-O$_2$ batteries which typically show a charge voltage above 4.0 V, 50% of electric energy

can be saved thus realizing the electrical energy saving. The reduction on charge volatge support for our proposed mechanism, indicating the efficient absorption of solar energy. This is ascribe to the photoexcited electron-hole pairs contribute to the electrochemical reactions at both electrodes. Thus the photovoltage on ZnS photocatalyst is effectively employed to reduce the charge voltage input. As a result, the photo-driven charge strategy reveals as a feasible methode to lower the charge voltage of solid-state Li-O_2 batteries.
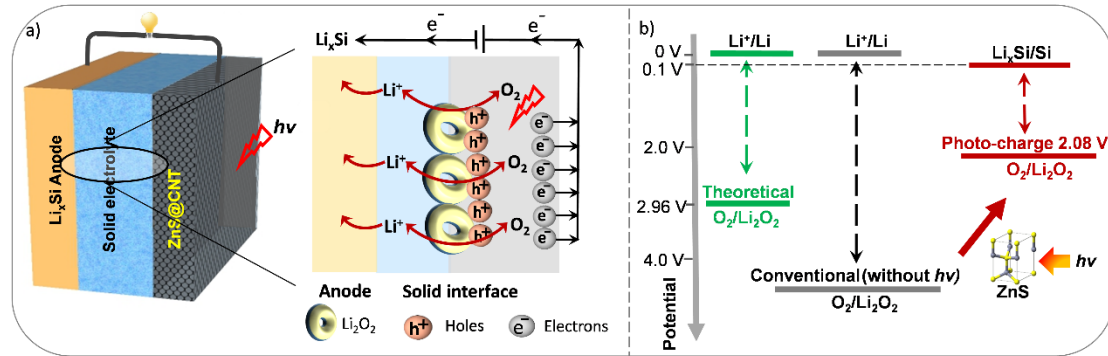
Fig. 4.1 (a) The illustration of photoassisted solid-state Li-ion O_2 battery. Magnified view: the photo-driven charge reaction at the solid electrolyte-electrode interface. (b) The comparison of charge voltages between conventional solid-state Li-O_2 battery and photoassisted solid-state Li-ion O_2 battery.

Fig. 4.2 illustrates the reaction mechanism for photo-driven solid-state Li-ion O_2 battery. The discharge process is primarily similar with that of typical Li-O_2 battery with Li_2O_2 as the discharge products, according to the following Equation (1):

$$2Li_xSi + xO_2 \rightarrow xLi_2O_2 + 2Si \tag{1}$$

However the charge process is relatively different, the magnified view in Fig. 4.1a gives more details for photo-driven Li_2O_2 oxidation at the solid electrolyte-electrode interface. Photoexcited electron-hole pairs would generated on ZnS upon excited by hv. Subsequently, the photogenerated holes would aid Li_2O_2 oxidation due to its highly oxidative reactivity. This reaction proceeds under the driving force between VB level of ZnS photocatalyst and O_2/Li_2O_2 couple potential. At the same time, the photogenerated electrons in the CB would migrate to the anode along external circuit, aiding the Li^+ ions insertion into Si, based on the following Equation(2), (3) and (4).

$$\text{Photocatalyst} \xrightarrow{hv} e^- + h^+ \tag{2}$$

$$\text{Cathode: } 2h^+ + Li_2O_2 \rightarrow 2Li^+ + O_2 \tag{3}$$

$$\text{Anode: } xe^- + xLi^+ + Si \rightarrow Li_xSi \tag{4}$$

In the photo-driven charge pathway, the absorbed solar energy is used compensate the electrical energy input, thus resulting as the reduction on charge voltage. Based on the energy diagram, the electrons are elevated to higher energy level by using solar energy, and the ZnS photocatalyst enables the photoassisted solid-state Li-ion O_2 battery charged at 1.9 V in theoretical.
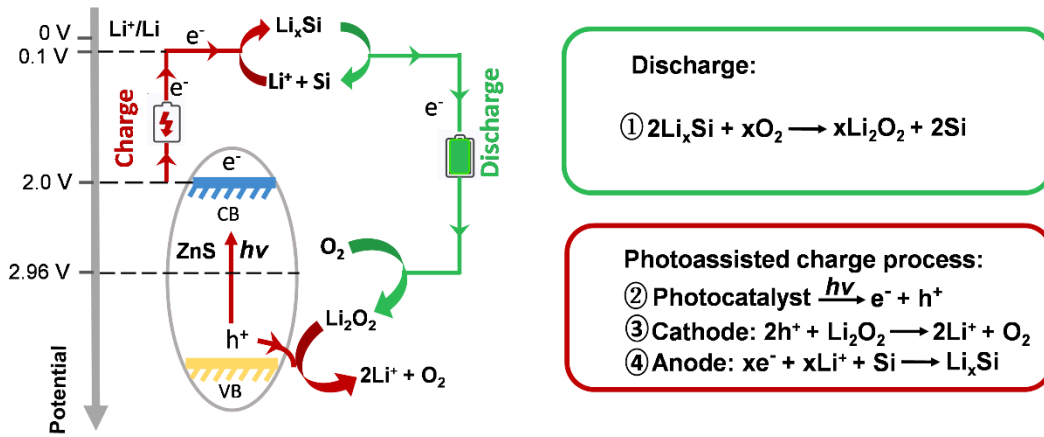
Fig. 4.2 Energy diagram for the solar battery integrated with a ZnS photoelectrode.

After the battery assembly, a typically high charge voltage of 4.09 V is acquired at 0.026 mA cm^{-2}. In contrast, the charge voltage of solid-state Li-ion O_2 battery under irradiation is distinctly decreased to 2.08 V, as displayed in Fig. 4.3a. The resultant photoassisted charge voltage is in good agreement with theoretical speculation of 1.9 V, which is considered to potentially address the inherent defect in solid-state Li-O_2 batteries. Furthermore, the charge voltage (2.08 V) is nearly one times lower compared with conventional solid battery (> 4.0 V), and thereby largely improves energy conversion efficiency. The rate capability are exhibited in Fig. 4.3b and c. Although the profile trend on charge slightly rises because of the increasingly large interfacial resistance at high rate. While the resultant charge voltage is 2.5 V at 0.20 mA cm^{-2}

which is much lower than that of conventional batteries. The cycling ability of both common and photo-driven solid-state Li-ion O_2 batteries were investigated to provide more comprehensive comparison.
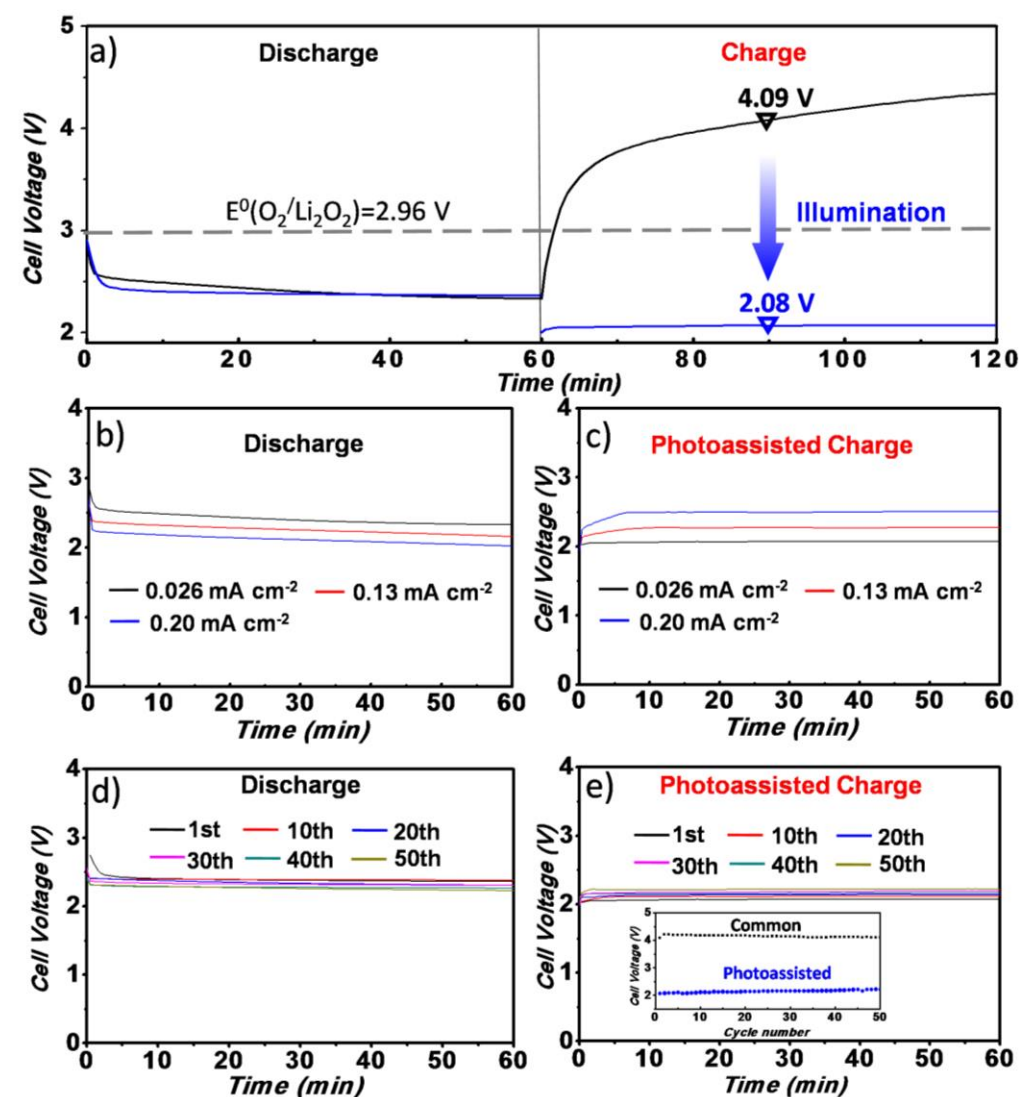
Fig. 4.3 (a) The comparison on the charge/discharge profiles of the solid-state Li-ion O_2 battery with and without irradiation at 0.026 mA cm^{-2}. (b), (c) The rate capability of solid-state Li-ion O_2 battery at various current densities. (d), (e) The discharge and photoassisted charge profiles of the solid-state Li-ion O_2 battery at 0.026 mA cm^{-2}. Insert: The comparison on charge voltage between photoassisted and common solid Li-ion O_2 batteries.

As presented in Fig. 4.3d and e, the charge voltage of photoassisted solid-state battery are kept stable at ~ 2.2 V after 50 cycles. From the comparison with common solid-state Li-ion O_2 battery (inserted in Fig. 4.3d), the introduction of solar energy into solid-state Li-O_2 batteries can resolve the overvoltage issue and thereby elevate the electric energy efficiency, which indicates the pivotal role of photo-driven Li_2O_2 oxidation for high battery reversibility.

More details for the discharge/charge products are presented as Raman spectra, which is obtained after discharge and photoassisted charge processes at 0.026 mA cm^{-2} for 1 h. As can be seen in Fig. 4.4a, the typical peak variation is well assigned to the formation/decomposition of Li_2O_2 during discharge/charge. The results demonstrate that Li_2O_2 dominates the main discharge product, which can be completely decomposed in the proposed photo-driven charge process. Additionally, the morphology of discharge/charge products are collected by transmission electron microscopy (TEM). Before discharge, it can be observed ZnS photocatalyst particles composed of fine grains, which is favorable for the photoexcited carriers transportation from inside to surface of ZnS photoelectrode, enhancing the photocatalysis activity. After discharge, instead of the classic toroidal-morphology of Li_2O_2,[181; 182] the layer products evenly covered on the surface of ZnS@CNT cathode can be clearly observed, which is similar to the previous results.[183] The thin layer structure could provide plentiful active reaction sites for Li_2O_2 particles and photogenerated holes, and contribute to the efficient Li_2O_2 decomposition under illumination. Subsequently, the resultant thin layer completely disappears after photo-driven Li_2O_2 oxidation process. This TEM result, together with Raman analysis, evidences the proposed photo-electrochemical reaction and the feasibility of photo-driven Li_2O_2 oxidation strategy in solid Li-O_2 battery.[183]
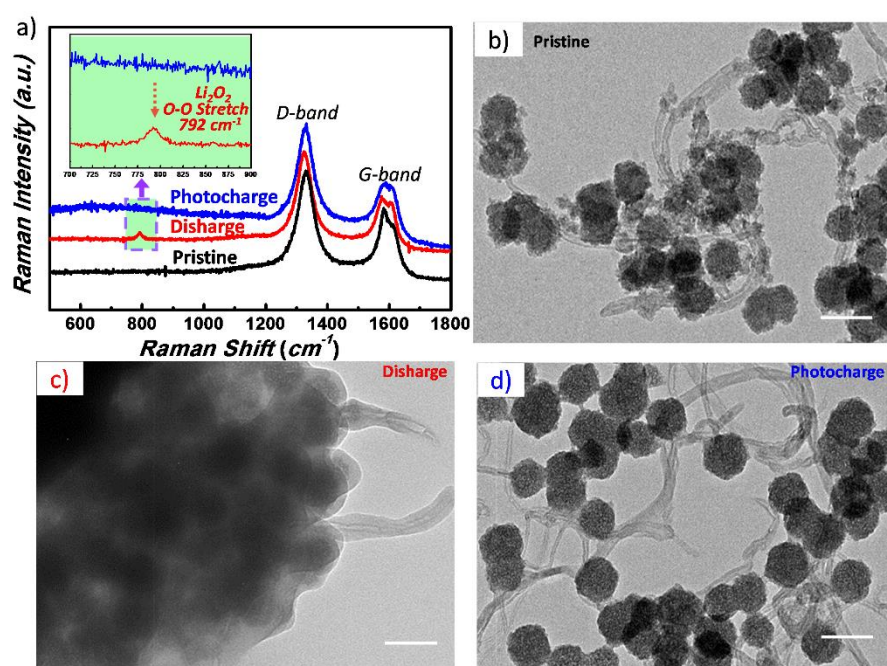
Fig. 4.4 (a) Ex-situ Raman spectra of cathodes analyzed at pristine, after discharge and after photoassisted charge processes. TEM images of cathodes observed at pristine (b), after discharge (c) and after photoassisted charge processes (d), scale baris 100 nm.

Thanks to the high ionic conductivity and plasticity, the plastic-crystalline electrolyte could enable the proposed solid-state Li-O_2 battery to be potentially flexible. In order to verify its future application on flexible/wearable electronic devices, a bendable solid-state Li-O_2 battery is proposed and realized, as illustrate in Fig. 4.5a. The assembled battery can successfully power light-emitting-diode (LED) under externally bendable condition (Fig. 4.5b). As expected, the bendable cell presents a low charge plateau of 2.15 V under illumination and favorable cycling performance (Figure 5c and d), which well maintains the superior electrical energy efficiency under bending state. Upon charging at a high current density of 0.13 mA cm^{-2}, the battery voltage could be controlled within 2.48 V. It is noted such a voltage is still much lower than that of any other traditional Li-O_2 batteries without irradiation, as shown in Fig. 4.5e. Based on above results, this proposed solid-state Li-O_2 battery shows appealing potential on flexible/wearable electronic devices.
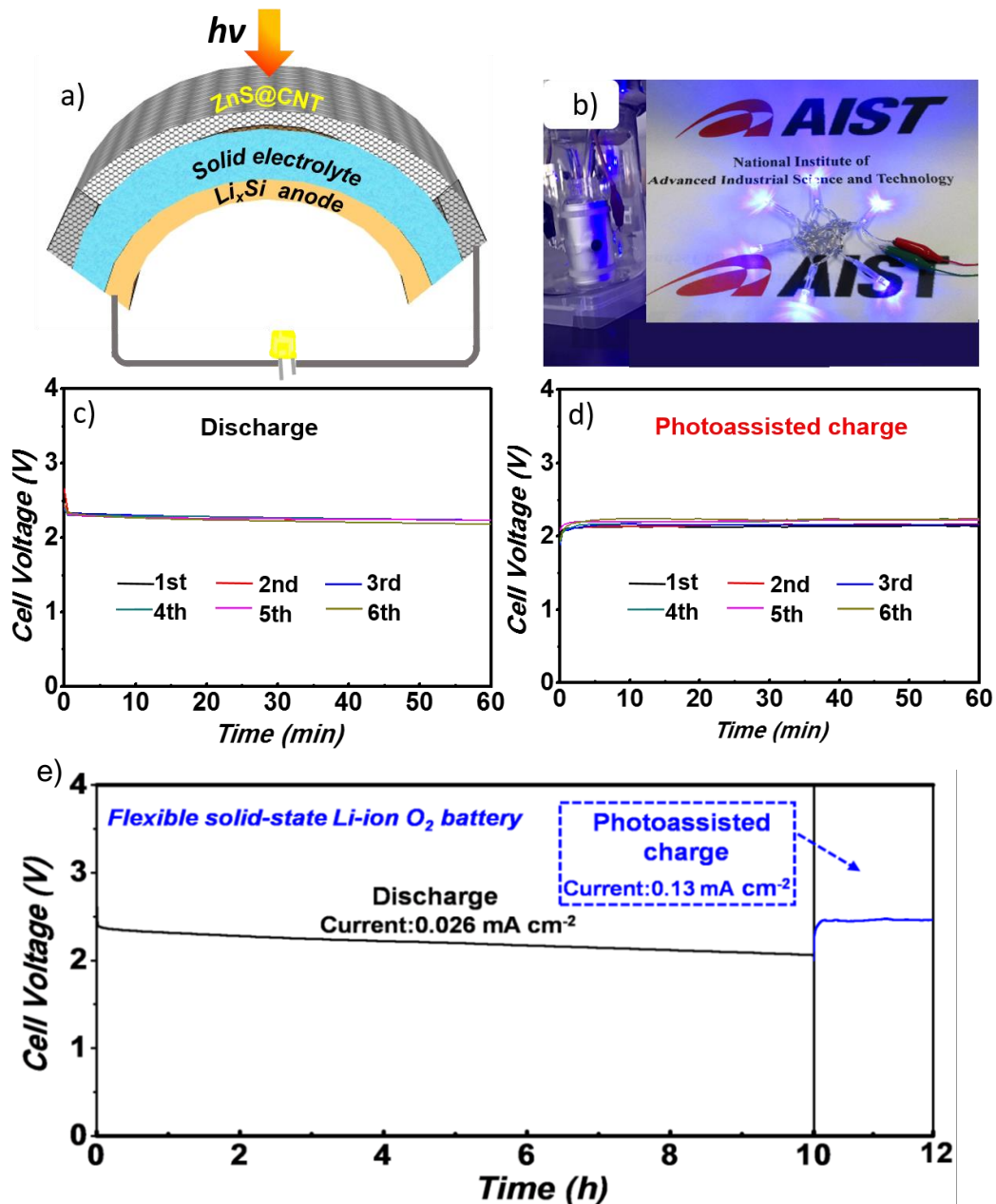
Fig. 4.5 (a) Schematic illustration of the proposed flexible photoassisted solid Li-ion O_2 battery. (b) Digital image of the assembled flexible solid Li-ion O_2 battery powering LED lamps. (c), (d) The discharge and photoassisted charge profiles of the flexible battery at 0.026 mA cm^{-2}. (e) The discharge profile of flexible photoassisted-solid battery at 0.026 mA cm^{-2} for 10 h and photoassisted charge profile at 0.13 mA cm^{-2} for 2 h.

4.4 Conclusions

Although solid-state Li-O$_2$ battery shows attractive improvement on safety, the lack of success should be ascribed to the sluggish reaction arising from solid-solid interface. In conclusion, a new energy conversion and storage device integrated solar energy with solid Li-O$_2$ battery is proposed and achieved. By employing a ZnS photocatalyst to capture solar energy, the charge voltage of solid Li-ion O$_2$ battery can be successfully decreased to 2.08 V, even lower than the discharge voltage. Such a low charge voltage directly leads to an ultrahigh energy efficiency of 113%, which is corresponding to electric energy saving of ~50%. Different from conventional solid Li-O$_2$ batteries, the proposed photo-driven device can output more electric electric energy (discharge/) than input (charge). This work validates an attractive strategy to solve the pressing challenge derived from large interfacial resistance in solid-state Li-O$_2$ battery. From a broader perspective, this work also demonstrates an attractive route to achieve solar energy conversion and storage in solid-state Li-O$_2$ battery.

Chapter 5 Conclusions

In summary, preliminary studies on Li-air batteries do suggest the promise to offer much higher gravimetric energy densities than currently achievable. In practical, several key obstacles must be resolved before the promise becomes a reality, such as high charge potential, low round-trip efficiency, poor cyclability and the safety issue arising from the organic electrolyte. Among these drawbacks, the high charge overpotential has been considered as the central problem. In this research work, we therefore focus on the charge overpotential issue and propose to integrate a photocatlyst into nonaqueous Li-O_2 batteries for absorbing solar energy. The primary conclusions are generalized as follows:

In Chapter 2, C_3N_4 photocatalyst was synthesized and used not only as a photoelectrode but also as an oxygen electrode for the oxygen reduction reaction. A photoassisted rechargeable Li-O_2 battery based on C_3N_4 photocatalyst coupled with LiI redox mediator has been successfully proposed and realized. In the photoassisted battery, during charging under solar illumination, the I^- ions in the electrolyte can readily be oxidized to I_3^- ions by photogenerated holes from C_3N_4 photocatalyst. Subsequently, the I_3^- ions would transfer to the air electrode side and decompose Li_2O_2 releasing Li^+ ions and O_2. Meanwhile, freed from the Coulomb absorption of holes, photogenerated electrons from C_3N_4 photocatalyst move to the anode side reducing Li^+ to Li thus completing the whole charge process. During this photo-oxidative reaction, both of the photoexcited electron-hole pairs participate the charge reaction, and thereby solar energy is captured by C_3N_4 photocatalyst and stored as electrochemical energy in the Li-O_2 battery. Namely, the photovoltage generated on the g-C_3N_4 photoelectrode compensates the required charge voltage. Finally, the charging voltage of Li-O_2 battery is decreased to 1.9 V, the lowest value for charge process to date, which is significantly lower than that of any other conventional Li–O_2 batteries. It is also noted that the charging voltage (~1.9 V) is even lower than the discharging voltage (~2.7 V), leading to an electric energy efficiency of 142%. This work effciciently addresses the charge

overpotential issue in nonaqueous Li-O$_2$ battery. Simultaneously, it provides a promising avenue to achieve solar energy conversion and storage in a high energy-density Li-O$_2$ battery.

Chapter 3: Substantial efforts have been devoted to reduce the charge overpotentials. In addition, photocharging rechargeable batteries reported to date have generally employ liquid redox mediators as either the electron–hole transfer agent or catholyte/anolyte. Although the redox mediators have become focal points in rechargeable Li-O$_2$ battery research for reducing the charge overpotential, serious shuttle effect and side reaction related to redox mediator have been discovered. This directly leads to the loss of both the RM content and electrical energy efficiency and displays as trend in increase of charge voltage and the deterioration of the cycling performance. This phenomenon has been further evidenced by FTIR measurement in our work. In this respect, removing the LiI redox mediator, an unmediated photoelectrochemical method is successfully demonstrated. We then construct a photoassisted Li-O$_2$ battery based on the direct photo-oxidative reaction of solid Li$_2$O$_2$ by photoexcited holes derived from the C$_3$N$_4$ photoelectrode. With the aid of solar energy, we here reduced the charge voltage of the Li–O$_2$ battery to 1.96 V without using any RM. The direct photo-oxidation reaction of Li$_2$O$_2$ products is illustrated by XRD and SEM measurements. We demonstrate an unmediated photoelectrochemical approach to effectively address the overpotential issue in Li– O$_2$ batteries. As a result, the electrical energy efficiency and the cycling stability of the Li -O$_2$ batteries were enhanced greatly by avoiding the side reaction. More importantly, owing to the poor photo/thermal stability of the liquid organic electrolyte under irradiation, all-solid-state batteries is regarded as an attractive alternative for photocharging energy storage systems. Our unmediated photoelectrochemical oxidation approach may provide a promising avenue for the further design of photocharging all-solid-state batteries. Through this work, we improve the shortcomings in our former work, meanwhile, guide a promising direction for the future development of photo-solid-state batteries.

Chapter 4: Although the solid-state Li-O$_2$ battery with high energy-density and

enhanced safety shows appealing potential for electric vehicles applications. It is well known that the challenge of high charge overpotential is even more serious on solid-state systems. The lack of success in solid-state Li-O$_2$ batteries is attributed to high charge overpotential derived from the solid-solid interface, which has become the main bottleneck for further advance of solid-state Li-O$_2$ battery. Based on our previous results, the incorporation of solar energy with solid-state Li-O$_2$ battery is applied and effectively decrease the charge voltage of solid-state Li-O$_2$ battery. Accordingly, a photo-assisted solid Li-O$_2$ battery is designed and fabricated. In this work, due to the suitable band positions, ZnS is chosen as the photocatalyst to realize the photo-driven solid-state Li-O$_2$ batteries. Finally, the ZnS@CNT composite is used as an oxygen electrode and a photoelectrode simultaneously. Additionally, instead of Li metal anode, lithiated silicon (Li$_x$Si) is employed as the anode for the safety improvement in the proposed solid-state Li-ion O$_2$ battery. Owing to the high ionic conductivity ($\sim$ 3 mS cm^{-1} at 25 °C) and plasticity, a 5 mol% LiTFSI dissolved in plastic-crystal form of succinonitrile (SCN) was utilized as the solid electrolyte. Under the assistance of photogenerated carriers, the rate-determining step of charge transfer for the Li$_2$O$_2$ oxidation is largely facilitated, enabling a favorable kinetics for oxygen evolution reaction at the solid-solid interface. The proposed photoassisted strategy endows the solid-state Li-O$_2$ battery with a low charge voltage of 2.08 V and high electric energy efficiency. The cyclability of common and photoassisted solid-state Li-ion O$_2$ batteries were both investigated at 0.026 mA cm^{-2}. The charging voltage of photoassisted solid-state Li-ion O$_2$ battery can keep stable at around 2.2 V after 50 repeated cycles. Compared with solid-state Li-ion O$_2$ battery without illumination, the introduction of solar energy into solid-state Li-ion O$_2$ batteries can effectively address the overpotential issue arising from the large interfacial resistance.

In this article, the photoassisted charge strategy are integrated with three types of Li-O$_2$ batteries, that is, 1) Nonaqueous Li-O$_2$ battery with redox mediator, 2) Nonaqueous Li-O$_2$ battery 3) Solid-state Li-O$_2$ battery. Next, the application on each battery system would be discussed and assessed. For the Li-O$_2$ battery with redox mediator, taking LiI

as an example, it serves as the soluble agent transferring between Li_2O_2 and cathode. The photoassisted charge strategy coupled redox mediator with photocatalyst is validated to be effective on Li_2O_2 decomposition. Benefit from the solubility and diffusivity, the redox mediator can reach the interior of cathode, and thus promote the contact with both Li_2O_2 and photocatalyst. Different from immobile catalysts, the diffusible redox mediator is more capable to completely catalyze the oxidation of Li_2O_2. Despite these advantage of redox mediator, its detrimental effect of shuttle reaction is discovered. Accordingly, the unmediated photoassisted charge is proposed and achieved by designing a proper coating structure of air electrode. Thus the photoassisted charge is applied on simple $Li-O_2$ battery due to the absence of redox mediator. The battery performance has been boosted by stabilizing the component. The simplified device also implies more application potential from views of cost and stability. For the photoassisted charge strategy, replacing organic liquid electrolyte with solid electrolyte can improve safety from the root, because the solid electrolyte shows negligible thermal instability under illumination. Integration of solar energy with solid $Li-O_2$ battery would be more attractive compared with aprotic $Li-O_2$ batteries due to the favorable safety, which is the critical factor for practical implementation.

Although promising, to fully develop the photo-charge energy storage systems, challenges will be to achieve real scientific and technological breakthroughs in energy density improvement, stable electrolytes discoveries and operation feasibility. Substantial research efforts are still required. Last but not the least, a long-standing hurdle is how to transform a $Li-O_2$ battery to a 'real' Li-air battery, which can be operated in the surrounding air. Through the efficient combination with solar energy, we are confident to realize a high-efficiency lithium–air batteries with long-lived practice application in future.

List of research results

JOURNAL PAPER

First author

[1] **Yang Liu,** Na Li, Shichao Wu, Kaiming Liao, Kai Zhu, Jin Yi and Haoshen Zhou, Reducing the charging voltage of a Li–O$_2$ battery to 1.9 V by incorporating a photocatalyst, ***Energy Environ. Sci.,*** 2015, 8, 2664—2667

[2] **Yang Liu,** Na Li, Kaiming Liao, Qi Li, Masayoshi Ishida and Haoshen Zhou, Lowering charge voltage of Li-O$_2$ batteries via an unmediated photoelectrochemical oxidation approach, ***J. Mater. Chem. A,*** 2016, 4, 12411–12415

[3] **Yang Liu**, Jin Yi, Yu Qiao, Di Wang, Ping He, Qi Li, Shichao Wu, Haoshen Zhou, Solar-driven efficient Li$_2$O$_2$ oxidation in solid-state Li-ion O$_2$ batteries, submitted to ***Energy Storage Mater.***

Co-authored

[4] Qi Li[1], **Yang Liu[1]**, Shaohua Guo, Haoshen Zhou, Solar energy storage in the rechargeable batteries, submitted to ***Nano. Today***

[5] Jin Yi, **Yang Liu**, Yu Qiao, Ping He, and Haoshen Zhou, Boosting the Cycle Life of Li–O$_2$ Batteries at Elevated Temperature by Employing a Hybrid Polymer–Ceramic Solid Electrolyte, ***ACS Energy Letters***, 2, 1378–1384, May, 2017

[6] Qi Li, Na Li, **Yang Liu**, Yarong Wang, and Haoshen Zhou, high-Safety and low-cost photoassisted chargeable aqueous sodium-ion batteries with 90% input electric energy savings, ***Adv. Energy Mater.*** 2016, 1600632.

[7] Shichao Wu, Jin Yi, Kai Zhu, Songyan Bai, **Yang Liu**, Yu Qiao, Masayoshi Ishida, and Haoshen Zhou, A super-hydrophobic quasi-solid electrolyte for Li-O$_2$ battery with improved safety and cycle life humid atmosphere, ***Adv. Energy Mater.***

2016,1601759

[8] Jin Yi, Shichao Wu, Songyan Bai, **Yang Liu**, Na Li and Haoshen Zhou, Interfacial construction of Li_2O_2 for a performance-improved polymer Li–O_2 battery, *J. Mater. Chem. A*, 2016, 4, 2403-2407

PRESENTATION

Yang Liu, Haoshen Zhou, Lowering the charge voltage of Li-O_2 battery system by incorporating a C_3N_4 photocatalyst, 2016 International Conference on Green Energy and Applications, Singapore, March 23-24, 2016 (oral).

Acknowledgments

The scenes that, for the first time, I come to Japan and start the Ph.D. study in University of Tsukuba is just happened yesterday. At this very moment, I am about to graduate and obtain the doctoral degree. This would become the most important and memorable moment in my whole life. I owe my gratitude to all those people who have given me help, guidance and encourage and because of whom my doctoral career has been the most valuable wealth.

First and Foremost, I would like to express my sincere gratitude to Prof. Haoshen Zhou. Under his assistance, I gained the oppotunity to pursue a Ph.D.degree in University of Tsukuba. His encouragement and guidance help me walked through all the stages of my Ph.D. study. He could always give me instructive advice and useful suggestions on my research, which means a lot to me. What impressed me most is his strict research attitude and creative thought. It is very lucky to study with such a knowledgeable and approachable teacher during Ph.D. period.

I would like to express my sincere thanks to my vice-supervisor Prof. Masayoshi Ishida and Assistant Prof. Hanada at University of Tsukuba. They are quite affable and patient people. They gave me unselfish assistance in my daily life and research work when I need help. I have enjoyed a good time when joining the party in Ishida's lab. I am really pleased for their enthusiastic invitations. Special gratitude is expressed to Prof. Keiichi Okajima and Associate Prof. Hirohisa Aki for their encouragement and kind help.

My heartfelt gratitude goes to Mr. J. Okagaki, Dr. H. Kitaura, Dr. E. Hosono, Dr. H. Matsuda and Dr. T. Saito in Energy Interface Technology Research Group at AIST. I want to express the special thanks to Dr. E. Yoo, for her nice help and suggestion for my graduation defense.

I would further like to express my special appreciation to Dr. Na Li and Dr. Jin Yi. I learned a lot experimental techniques and theoretical knowledge from Dr. Na Li. She is

the people to help me enter the research field of Li-O$_2$ batteries. I will always remember her kindness, guidance and strongly support. Dr. Jin Yi share many invaluable suggestions and experiences on improving the experiment results and making a good manuscript. His patience and useful advice assist me overcome a series of difficulties in scientific research.

Many thanks to Dr. Shichao Wu and he taught me many basic experiment technique, from making electrode for Li-O2 battery to fabricating batteries and evaluating the battery performance. I really appreciate Dr. Kaiming Liao for the always useful information. I also feel grateful to Mr. Yu Qiao, who often provides help on Raman measurements. Additionally the discussion on the research study with Dr. Shichao Wu and Mr. Yu Qiao often inspired me and achieved lots of improvements. My sincere thanks would go to Dr. Kai Zhu, Dr. S. Bai and Ms. Q. Li. We almost come to Japan at same time and build deep friendship during the last three years. Many thanks to my dear friends and lab mates Dr. Shaohua. Guo Dr. Fujun Li and Dr. Xizheng Liu, Dr. Tao. Zhang, Dr. Yang. Sun, Dr. yarong Wang, Miss Yibo He and Mr. Xiang Li.

Last but not least, I would like to especially thank my family. To my husband- I feel very happy and grateful to be with you. We will make progress together both in life and scientific research. To my younger sister- Thanks for your concern and miss. To my parents- I am very lucky and happy to be your daughter and I will try my best to make you happy. Words alone cannot express how I appreciate for your encouragement and love.

References

[1] Choi N-S, Chen Z, Freunberger S A, et al. Challenges Facing Lithium Batteries and Electrical Double-Layer Capacitors[J]. Angewandte Chemie International Edition, 2012, 51(40): 9994-10024.

[2] Mahmoudzadeh M A, Usgaocar A R, Giorgio J, et al. A high energy density solar rechargeable redox battery[J]. Journal of Materials Chemistry A, 2016, 4(9): 3446-3452.

[3] Black R, Adams B, Nazar L. Non-Aqueous and Hybrid Li-O2 Batteries[J]. Advanced Energy Materials, 2012, 2(7): 801-815.

[4] Alarco P-J, Abu-Lebdeh Y, Abouimrane A, et al. The plastic-crystalline phase of succinonitrile as a universal matrix for solid-state ionic conductors[J]. Nat Mater, 2004, 3(7): 476-481.

[5] Etacheri V, Marom R, Elazari R, et al. Challenges in the development of advanced Li-ion batteries: a review[J]. Energy & Environmental Science, 2011, 4(9): 3243-3262.

[6] Ohta N, Takada K, Zhang L, et al. Enhancement of the High-Rate Capability of Solid-State Lithium Batteries by Nanoscale Interfacial Modification[J]. Advanced Materials, 2006, 18(17): 2226-2229.

[7] Lu L, Han X, Li J, et al. A review on the key issues for lithium-ion battery management in electric vehicles[J]. Journal of power sources, 2013, 226: 272-288.

[8] Doerffel D, Sharkh S A. A critical review of using the Peukert equation for determining the remaining capacity of lead-acid and lithium-ion batteries[J]. Journal of power sources, 2006, 155(2): 395-400.

[9] Li H, Wang Z, Chen L, et al. Research on Advanced Materials for Li-ion Batteries[J].

Advanced Materials, 2009, 21(45): 4593-4607.

[10] Du Pasquier A, Plitz I, Menocal S, et al. A comparative study of Li-ion battery, supercapacitor and nonaqueous asymmetric hybrid devices for automotive applications[J]. Journal of Power Sources, 2003, 115(1): 171-178.

[11] Palacin M R. Recent advances in rechargeable battery materials: a chemist's perspective[J]. Chemical Society Reviews, 2009, 38(9): 2565-2575.

[12] Thackeray M M, Wolverton C, Isaacs E D. Electrical energy storage for transportation—approaching the limits of, and going beyond, lithium-ion batteries[J]. Energy & Environmental Science, 2012, 5(7): 7854-7863.

[13] Yabuuchi N, Ohzuku T. Novel lithium insertion material of LiCo 1/3 Ni 1/3 Mn 1/3 O 2 for advanced lithium-ion batteries[J]. Journal of Power Sources, 2003, 119: 171-174.

[14] Lee J K, Smith K B, Hayner C M, et al. Silicon nanoparticles–graphene paper composites for Li ion battery anodes[J]. Chemical Communications, 2010, 46(12): 2025-2027.

[15] Wu H, Yu G, Pan L, et al. Stable Li-ion battery anodes by in-situ polymerization of conducting hydrogel to conformally coat silicon nanoparticles[J]. Nature communications, 2013, 4: 1943.

[16] Yoshio M, Wang H, Fukuda K, et al. Carbon-coated Si as a lithium-ion battery anode material[J]. Journal of The Electrochemical Society, 2002, 149(12): A1598-A1603.

[17] Cai Z, Liu Y, Liu S, et al. High performance of lithium-ion polymer battery based on non-aqueous lithiated perfluorinated sulfonic ion-exchange membranes[J]. Energy & Environmental Science, 2012, 5(2): 5690-5693.

[18] Bouchet R, Lascaud S, Rosso M. An EIS study of the anode Li/PEO-LiTFSI of a

Li polymer battery[J]. Journal of the electrochemical society, 2003, 150(10): A1385-A1389.

[19] Scrosati B, Croce F, Panero S. Progress in lithium polymer battery R&D[J]. Journal of power sources, 2001, 100(1): 93-100.

[20] Choi Y-J, Chung Y-D, Baek C-Y, et al. Effects of carbon coating on the electrochemical properties of sulfur cathode for lithium/sulfur cell[J]. Journal of Power Sources, 2008, 184(2): 548-552.

[21] Li N, Weng Z, Wang Y, et al. An aqueous dissolved polysulfide cathode for lithium-sulfur batteries[J]. Energy & Environmental Science, 2014, 7(10): 3307-3312.

[22] Li F, Zhang T, Zhou H. Challenges of non-aqueous Li–O 2 batteries: electrolytes, catalysts, and anodes[J]. Energy & Environmental Science, 2013, 6(4): 1125-1141.

[23] Liu N, Wu H, Mcdowell M T, et al. A yolk-shell design for stabilized and scalable Li-ion battery alloy anodes[J]. Nano letters, 2012, 12(6): 3315-3321.

[24] Girishkumar G, Mccloskey B, Luntz A, et al. Lithium− air battery: promise and challenges[J]. The Journal of Physical Chemistry Letters, 2010, 1(14): 2193-2203.

[25] Mizuno F, Nakanishi S, Kotani Y, et al. Rechargeable Li-air batteries with carbonate-based liquid electrolytes[J]. Electrochemistry, 2010, 78(5): 403-405.

[26] Xiao J, Mei D, Li X, et al. Hierarchically porous graphene as a lithium–air battery electrode[J]. Nano letters, 2011, 11(11): 5071-5078.

[27] Wang Y, Zhou H. A lithium-air battery with a potential to continuously reduce O 2 from air for delivering energy[J]. Journal of Power Sources, 2010, 195(1): 358-361.

[28] Kumar B, Kumar J, Leese R, et al. A solid-state, rechargeable, long cycle life

lithium–air battery[J]. Journal of The Electrochemical Society, 2010, 157(1): A50-A54.

[29] Zheng J P, Liang R Y, Hendrickson M, et al. Theoretical Energy Density of Li–Air Batteries[J]. Journal of The Electrochemical Society, 2008, 155(6): A432-A437.

[30] Lim H-D, Song H, Gwon H, et al. A new catalyst-embedded hierarchical air electrode for high-performance Li–O 2 batteries[J]. Energy & Environmental Science, 2013, 6(12): 3570-3575.

[31] Xu J-J, Wang Z-L, Xu D, et al. Tailoring deposition and morphology of discharge products towards high-rate and long-life lithium-oxygen batteries[J]. Nature communications, 2013, 4.

[32] Zhu X, Zhao T, Wei Z, et al. A high-rate and long cycle life solid-state lithium–air battery[J]. Energy & Environmental Science, 2015, 8(12): 3745-3754.

[33] Kim H, Lim H-D, Kim J, et al. Graphene for advanced Li/S and Li/air batteries[J]. Journal of Materials Chemistry A, 2014, 2(1): 33-47.

[34] Ottakam Thotiyl M M, Freunberger S A, Peng Z, et al. The carbon electrode in nonaqueous Li–O2 cells[J]. Journal of the American Chemical Society, 2012, 135(1): 494-500.

[35] Lu Y-C, Kwabi D G, Yao K P, et al. The discharge rate capability of rechargeable Li–O 2 batteries[J]. Energy & Environmental Science, 2011, 4(8): 2999-3007.

[36] Guo Z, Wang J, Wang F, et al. Leaf-like Graphene Oxide with a Carbon Nanotube Midrib and Its Application in Energy Storage Devices[J]. Advanced Functional Materials, 2013, 23(38): 4840-4846.

[37] Wu S, Tang J, Li F, et al. Low charge overpotentials in lithium–oxygen batteries based on tetraglyme electrolytes with a limited amount of water[J]. Chemical Communications, 2015, 51(94): 16860-16863.

[38] Li L, Chai S-H, Dai S, et al. Advanced hybrid Li–air batteries with high-performance mesoporous nanocatalysts[J]. Energy & Environmental Science, 2014, 7(8): 2630-2636.

[39] Bryantsev V S, Giordani V, Walker W, et al. Predicting solvent stability in aprotic electrolyte Li–air batteries: nucleophilic substitution by the superoxide anion radical (O2•–)[J]. The Journal of Physical Chemistry A, 2011, 115(44): 12399-12409.

[40] Thotiyl M M O, Freunberger S A, Peng Z, et al. A stable cathode for the aprotic Li–O2 battery[J]. Nature materials, 2013, 12(11): 1050-1056.

[41] Freunberger S A, Chen Y, Drewett N E, et al. The Lithium–Oxygen Battery with Ether-Based Electrolytes[J]. Angewandte Chemie International Edition, 2011, 50(37): 8609-8613.

[42] Itkis D M, Semenenko D A, Kataev E Y, et al. Reactivity of carbon in lithium–oxygen battery positive electrodes[J]. Nano letters, 2013, 13(10): 4697-4701.

[43] Zhong L, Mitchell R R, Liu Y, et al. In situ transmission electron microscopy observations of electrochemical oxidation of Li2O2[J]. Nano letters, 2013, 13(5): 2209-2214.

[44] Viswanathan V, Thygesen K S, Hummelshøj J, et al. Electrical conductivity in Li2O2 and its role in determining capacity limitations in non-aqueous Li-O2 batteries[J]. The Journal of chemical physics, 2011, 135(21): 214704.

[45] Ryu W-H, Yoon T-H, Song S H, et al. Bifunctional composite catalysts using Co3O4 nanofibers immobilized on nonoxidized graphene nanoflakes for high-capacity and long-cycle Li–O2 batteries[J]. Nano letters, 2013, 13(9): 4190-4197.

[46] Zhang T, Zhou H. From Li–O2 to Li–air batteries: Carbon nanotubes/ionic liquid gels with a tricontinuous passage of electrons, ions, and oxygen[J]. Angewandte

Chemie, 2012, 124(44): 11224-11229.

[47] Peng Z, Freunberger S A, Hardwick L J, et al. Oxygen reactions in a non-aqueous Li+ electrolyte[J]. Angewandte Chemie, 2011, 123(28): 6475-6479.

[48] Lu Y-C, Gasteiger H A, Parent M C, et al. The influence of catalysts on discharge and charge voltages of rechargeable Li–oxygen batteries[J]. Electrochemical and Solid-State Letters, 2010, 13(6): A69-A72.

[49] Lu Y-C, Xu Z, Gasteiger H A, et al. Platinum− gold nanoparticles: a highly active bifunctional electrocatalyst for rechargeable lithium− air batteries[J]. Journal of the American Chemical Society, 2010, 132(35): 12170-12171.

[50] Thapa A K, Saimen K, Ishihara T. Pd/MnO2 air electrode catalyst for rechargeable lithium/air battery[J]. Electrochemical and Solid-State Letters, 2010, 13(11): A165-A167.

[51] Li F, Tang D-M, Chen Y, et al. Ru/ITO: a carbon-free cathode for nonaqueous Li– O2 battery[J]. Nano letters, 2013, 13(10): 4702-4707.

[52] Yilmaz E, Yogi C, Yamanaka K, et al. Promoting formation of noncrystalline Li2O2 in the Li–O2 battery with RuO2 nanoparticles[J]. Nano letters, 2013, 13(10): 4679-4684.

[53] Guo Z, Zhou D, Liu H, et al. Synthesis of ruthenium oxide coated ordered mesoporous carbon nanofiber arrays as a catalyst for lithium oxygen battery[J]. Journal of Power Sources, 2015, 276: 181-188.

[54] Lu J, Lei Y, Lau K C, et al. A nanostructured cathode architecture for low charge overpotential in lithium-oxygen batteries[J]. Nature communications, 2013, 4.

[55] Zhang D, Fu Z, Wei Z, et al. Polarization of oxygen electrode in rechargeable lithium oxygen batteries[J]. Journal of the Electrochemical Society, 2010, 157(3): A362-A365.

[56] Peng Z, Freunberger S A, Chen Y, et al. A reversible and higher-rate Li-O2 battery[J]. Science, 2012, 337(6094): 563-566.

[57] Thapa A K, Ishihara T. Mesoporous α-MnO 2/Pd catalyst air electrode for rechargeable lithium–air battery[J]. Journal of Power Sources, 2011, 196(16): 7016-7020.

[58] Jung H-G, Jeong Y S, Park J-B, et al. Ruthenium-based electrocatalysts supported on reduced graphene oxide for lithium-air batteries[J]. Acs Nano, 2013, 7(4): 3532-3539.

[59] Dong S, Chen X, Zhang K, et al. Molybdenum nitride based hybrid cathode for rechargeable lithium–O 2 batteries[J]. Chemical Communications, 2011, 47(40): 11291-11293.

[60] Wang L, Zhao X, Lu Y, et al. CoMn2O4 spinel nanoparticles grown on graphene as bifunctional catalyst for lithium-air batteries[J]. Journal of The Electrochemical Society, 2011, 158(12): A1379-A1382.

[61] Shui J-L, Karan N K, Balasubramanian M, et al. Fe/N/C composite in Li–O2 battery: studies of catalytic structure and activity toward oxygen evolution reaction[J]. Journal of the American Chemical Society, 2012, 134(40): 16654-16661.

[62] Li F, Ohnishi R, Yamada Y, et al. Carbon supported TiN nanoparticles: an efficient bifunctional catalyst for non-aqueous Li–O 2 batteries[J]. Chemical Communications, 2013, 49(12): 1175-1177.

[63] Park C S, Kim K S, Park Y J. Carbon-sphere/Co 3 O 4 nanocomposite catalysts for effective air electrode in Li/air batteries[J]. Journal of Power Sources, 2013, 244: 72-79.

[64] Tang J, Wu S, Wang T, et al. Cage-Type Highly Graphic Porous Carbon–Co3O4

Polyhedron as the Cathode of Lithium–Oxygen Batteries[J]. ACS applied materials & interfaces, 2016, 8(4): 2796-2804.

[65] Kwak W-J, Lau K C, Shin C-D, et al. A Mo2C/carbon nanotube composite cathode for lithium–oxygen batteries with high energy efficiency and long cycle life[J]. ACS nano, 2015, 9(4): 4129-4137.

[66] Xu J J, Xu D, Wang Z L, et al. Synthesis of perovskite-based porous La0. 75Sr0. 25MnO3 nanotubes as a highly efficient electrocatalyst for rechargeable lithium–oxygen batteries[J]. Angewandte Chemie International Edition, 2013, 52(14): 3887-3890.

[67] Wang L, Ara M, Wadumesthrige K, et al. Graphene nanosheet supported bifunctional catalyst for high cycle life Li-air batteries[J]. Journal of Power Sources, 2013, 234: 8-15.

[68] Oh S H, Black R, Pomerantseva E, et al. Synthesis of a metallic mesoporous pyrochlore as a catalyst for lithium–O2 batteries[J]. Nature chemistry, 2012, 4(12): 1004-1010.

[69] Liang Z, Lu Y-C. Critical Role of Redox Mediator in Suppressing Charging Instabilities of Lithium–Oxygen Batteries[J]. Journal of the American Chemical Society, 2016, 138(24): 7574-7583.

[70] Lim H-D, Lee B, Zheng Y, et al. Rational design of redox mediators for advanced Li–O2 batteries[J]. Nature Energy, 2016, 1: 16066.

[71] Chen Y, Freunberger S A, Peng Z, et al. Charging a Li–O2 battery using a redox mediator[J]. Nature chemistry, 2013, 5(6): 489-494.

[72] Chase G V, Zecevic S, Wesley T W, et al. Soluble oxygen evolving catalysts for rechargeable metal-air batteries. Google Patents, 2011.

[73] Sun B, Huang X, Chen S, et al. An optimized LiNO 3/DMSO electrolyte for high-

performance rechargeable Li–O 2 batteries[J]. Rsc Advances, 2014, 4(22): 11115-11120.

[74] Sharon D, Hirsberg D, Afri M, et al. Catalytic Behavior of Lithium Nitrate in Li-O2 Cells[J]. ACS applied materials & interfaces, 2015, 7(30): 16590-16600.

[75] Lim H D, Song H, Kim J, et al. Superior rechargeability and efficiency of lithium–oxygen batteries: hierarchical air electrode architecture combined with a soluble catalyst[J]. Angewandte Chemie International Edition, 2014, 53(15): 3926-3931.

[76] Yu M, Ren X, Ma L, et al. Integrating a redox-coupled dye-sensitized photoelectrode into a lithium–oxygen battery for photoassisted charging[J]. Nature communications, 2014, 5.

[77] Sun D, Shen Y, Zhang W, et al. A solution-phase bifunctional catalyst for lithium–oxygen batteries[J]. Journal of the American Chemical Society, 2014, 136(25): 8941-8946.

[78] Torres W R, Herrera S E, Tesio A Y, et al. Soluble TTF catalyst for the oxidation of cathode products in Li-Oxygen battery: A chemical scavenger[J]. Electrochimica Acta, 2015, 182: 1118-1123.

[79] Yang H, Wang Q, Zhang R, et al. The electrochemical behaviour of TTF in Li–O 2 batteries using a TEGDME-based electrolyte[J]. Chemical Communications, 2016, 52(48): 7580-7583.

[80] Bergner B J, SchüRmann A, Peppler K, et al. TEMPO: a mobile catalyst for rechargeable Li-O2 batteries[J]. Journal of the American Chemical Society, 2014, 136(42): 15054-15064.

[81] Bergner B J, Busche M R, Pinedo R, et al. How To Improve Capacity and Cycling Stability for Next Generation Li–O2 Batteries: Approach with a Solid Electrolyte and Elevated Redox Mediator Concentrations[J]. ACS applied materials &

interfaces, 2016, 8(12): 7756-7765.

[82] Lee C K, Park Y J. CsI as Multifunctional Redox Mediator for Enhanced Li–Air Batteries[J]. ACS applied materials & interfaces, 2016, 8(13): 8561-8567.

[83] Kundu D, Black R, Adams B, et al. A highly active low voltage redox mediator for enhanced rechargeability of lithium–oxygen batteries[J]. ACS central science, 2015, 1(9): 510-515.

[84] Lu Y-C, Gallant B M, Kwabi D G, et al. Lithium–oxygen batteries: bridging mechanistic understanding and battery performance[J]. Energy & Environmental Science, 2013, 6(3): 750-768.

[85] Li F, Kitaura H, Zhou H. The pursuit of rechargeable solid-state Li–air batteries[J]. Energy & Environmental Science, 2013, 6(8): 2302-2311.

[86] Takada K, Ohta N, Zhang L, et al. Interfacial modification for high-power solid-state lithium batteries[J]. Solid State Ionics, 2008, 179(27): 1333-1337.

[87] Kitaura H, Zhou H. Electrochemical Performance of Solid-State Lithium–Air Batteries Using Carbon Nanotube Catalyst in the Air Electrode[J]. Advanced Energy Materials, 2012, 2(7): 889-894.

[88] Yi J, Guo S, He P, et al. Status and prospects of polymer electrolytes for solid-state Li–O 2 (air) batteries[J]. Energy & Environmental Science, 2017, 10(4): 860-884.

[89] Wu S, Yi J, Zhu K, et al. A Super-Hydrophobic Quasi-Solid Electrolyte for Li-O2 Battery with Improved Safety and Cycle Life in Humid Atmosphere[J]. Advanced Energy Materials, 2017, 7(4).

[90] Chai J, Liu Z, Ma J, et al. In Situ Generation of Poly (Vinylene Carbonate) Based Solid Electrolyte with Interfacial Stability for LiCoO2 Lithium Batteries[J]. Advanced Science, 2017, 4(2).

[91] Mccloskey B D, Scheffler R, Speidel A, et al. On the efficacy of electrocatalysis in nonaqueous Li–O2 batteries[J]. Journal of the American Chemical Society, 2011, 133(45): 18038-18041.

[92] Mitchell R R, Gallant B M, Thompson C V, et al. All-carbon-nanofiber electrodes for high-energy rechargeable Li–O 2 batteries[J]. Energy & Environmental Science, 2011, 4(8): 2952-2958.

[93] Gallant B M, Mitchell R R, Kwabi D G, et al. Chemical and morphological changes of Li–O2 battery electrodes upon cycling[J]. The Journal of Physical Chemistry C, 2012, 116(39): 20800-20805.

[94] Christensen J, Albertus P, Sanchez-Carrera R S, et al. A critical review of Li/air batteries[J]. Journal of the Electrochemical Society, 2011, 159(2): R1-R30.

[95] Jung J-W, Im H-G, Lee D, et al. Conducting Nanopaper: A Carbon-Free Cathode Platform for Li–O2 Batteries[J]. ACS Energy Letters, 2017, 2(3): 673-680.

[96] Park M, Sun H, Lee H, et al. Lithium-air batteries: Survey on the current status and perspectives towards automotive applications from a battery industry standpoint[J]. Advanced Energy Materials, 2012, 2(7): 780-800.

[97] Yang X-H, He P, Xia Y-Y. Preparation of mesocellular carbon foam and its application for lithium/oxygen battery[J]. Electrochemistry Communications, 2009, 11(6): 1127-1130.

[98] Zhang T, Zhou H. A reversible long-life lithium–air battery in ambient air[J]. Nature communications, 2013, 4: 1817.

[99] Shui J, Lin Y, Connell J W, et al. Nitrogen-Doped Holey Graphene for High-Performance Rechargeable Li–O2 Batteries[J]. ACS Energy Letters, 2016, 1(1): 260-265.

[100] Mo Y, Ong S P, Ceder G. First-principles study of the oxygen evolution reaction

of lithium peroxide in the lithium-air battery[J]. Physical Review B, 2011, 84(20): 205446.

[101] Laoire C, Mukerjee S, Plichta E J, et al. Rechargeable lithium/TEGDME-LiPF6∕O2 battery[J]. Journal of The Electrochemical Society, 2011, 158(3): A302-A308.

[102] Mccloskey B, Speidel A, Scheffler R, et al. Twin problems of interfacial carbonate formation in nonaqueous Li–O2 batteries[J]. The journal of physical chemistry letters, 2012, 3(8): 997-1001.

[103] Kang S J, Mori T, Narizuka S, et al. Deactivation of carbon electrode for elimination of carbon dioxide evolution from rechargeable lithium–oxygen cells[J]. Nature communications, 2014, 5.

[104] Gallagher K G, Goebel S, Greszler T, et al. Quantifying the promise of lithium–air batteries for electric vehicles[J]. Energy & Environmental Science, 2014, 7(5): 1555-1563.

[105] Liao K, Wang X, Sun Y, et al. An oxygen cathode with stable full discharge–charge capability based on 2D conducting oxide[J]. Energy & Environmental Science, 2015, 8(7): 1992-1997.

[106] Lee J-H, Black R, Popov G, et al. The role of vacancies and defects in Na 0.44 MnO 2 nanowire catalysts for lithium–oxygen batteries[J]. Energy & Environmental Science, 2012, 5(11): 9558-9565.

[107] Park H W, Lee D U, Nazar L F, et al. Oxygen reduction reaction using MnO2 nanotubes/nitrogen-doped exfoliated graphene hybrid catalyst for Li-O2 battery applications[J]. Journal of The Electrochemical Society, 2013, 160(2): A344-A350.

[108] Cao Y, Wei Z, He J, et al. α-MnO 2 nanorods grown in situ on graphene as catalysts for Li–O 2 batteries with excellent electrochemical performance[J].

Energy & Environmental Science, 2012, 5(12): 9765-9768.

[109] Lei Y, Lu J, Luo X, et al. Synthesis of porous carbon supported palladium nanoparticle catalysts by atomic layer deposition: application for rechargeable lithium–O2 battery[J]. Nano letters, 2013, 13(9): 4182-4189.

[110] Shui J, Du F, Xue C, et al. Vertically aligned N-doped coral-like carbon fiber arrays as efficient air electrodes for high-performance nonaqueous Li–O2 batteries[J]. ACS nano, 2014, 8(3): 3015-3022.

[111] Shiraishi Y, Kanazawa S, Sugano Y, et al. Highly selective production of hydrogen peroxide on graphitic carbon nitride (g-C3N4) photocatalyst activated by visible light[J]. ACS Catalysis, 2014, 4(3): 774-780.

[112] Xu J, Brenner T J, Chen Z, et al. Upconversion-agent induced improvement of g-C3N4 photocatalyst under visible light[J]. ACS applied materials & interfaces, 2014, 6(19): 16481-16486.

[113] Xiang Q, Yu J, Jaroniec M. Preparation and enhanced visible-light photocatalytic H2-production activity of graphene/C3N4 composites[J]. The Journal of Physical Chemistry C, 2011, 115(15): 7355-7363.

[114] Li Q, Li N, Ishida M, et al. Saving electric energy by integrating a photoelectrode into a Li-ion battery[J]. Journal of Materials Chemistry A, 2015, 3(42): 20903-20907.

[115] Nikiforidis G, Tajima K, Byon H R. High Energy Efficiency and Stability for Photoassisted Aqueous Lithium–Iodine Redox Batteries[J]. ACS Energy Letters, 2016, 1(4): 806-813.

[116] Yu M, Mcculloch W D, Beauchamp D R, et al. Aqueous lithium–iodine solar flow battery for the simultaneous conversion and storage of solar energy[J]. Journal of the American Chemical Society, 2015, 137(26): 8332-8335.

[117] Wang X, Maeda K, Thomas A, et al. A metal-free polymeric photocatalyst for hydrogen production from water under visible light[J]. Nature materials, 2009, 8(1): 76-80.

[118] Boschloo G, Hagfeldt A. Characteristics of the iodide/triiodide redox mediator in dye-sensitized solar cells[J]. Accounts of chemical research, 2009, 42(11): 1819-1826.

[119] Zhang J, Zhang M, Lin L, et al. Sol Processing of Conjugated Carbon Nitride Powders for Thin-Film Fabrication[J]. Angewandte Chemie, 2015, 127(21): 6395-6399.

[120] Niu P, Zhang L, Liu G, et al. Graphene-Like Carbon Nitride Nanosheets for Improved Photocatalytic Activities[J]. Advanced Functional Materials, 2012, 22(22): 4763-4770.

[121] Zhang J, Chen X, Takanabe K, et al. Synthesis of a Carbon Nitride Structure for Visible-Light Catalysis by Copolymerization[J]. Angewandte Chemie International Edition, 2010, 49(2): 441-444.

[122] Su F, Mathew S C, Lipner G, et al. mpg-C3N4-catalyzed selective oxidation of alcohols using O2 and visible light[J]. Journal of the American Chemical Society, 2010, 132(46): 16299-16301.

[123] Yi J, Liao K, Zhang C, et al. Facile in Situ Preparation of Graphitic-C3N4@ carbon Paper As an Efficient Metal-Free Cathode for Nonaqueous Li–O2 Battery[J]. ACS applied materials & interfaces, 2015, 7(20): 10823-10827.

[124] Luo W B, Chou S L, Wang J Z, et al. A Metal-Free, Free-Standing, Macroporous Graphene@ g-C3N4 Composite Air Electrode for High-Energy Lithium Oxygen Batteries[J]. Small, 2015, 11(23): 2817-2824.

[125] Ohno T, Mitsui T, Matsumura M. Photocatalytic activity of S-doped TiO2

photocatalyst under visible light[J]. Chemistry Letters, 2003, 32(4): 364-365.

[126] Iwasaki M, Hara M, Kawada H, et al. Cobalt ion-doped TiO2 photocatalyst response to visible light[J]. Journal of Colloid and Interface Science, 2000, 224(1): 202-204.

[127] Feng N, He P, Zhou H. Critical Challenges in Rechargeable Aprotic Li–O2 Batteries[J]. Advanced Energy Materials, 2016.

[128] Feng N, He P, Zhou H. Enabling catalytic oxidation of Li2O2 at the liquid–solid interface: the evolution of an aprotic Li–O2 battery[J]. ChemSusChem, 2015, 8(4): 600-602.

[129] Liu T, Leskes M, Yu W, et al. Cycling Li-O2 batteries via LiOH formation and decomposition[J]. Science, 2015, 350(6260): 530-533.

[130] Schaltin S, Vanhoutte G, Wu M, et al. A QCM study of ORR-OER and an in situ study of a redox mediator in DMSO for Li–O 2 batteries[J]. Physical Chemistry Chemical Physics, 2015, 17(19): 12575-12586.

[131] Wang Y, Xia Y. Li-O2 batteries: an agent for change[J]. Nature chemistry, 2013, 5(6): 445-447.

[132] Burke C M, Black R, Kochetkov I R, et al. Implications of 4 e– Oxygen Reduction via Iodide Redox Mediation in Li–O2 Batteries[J]. ACS Energy Letters, 2016, 1(4): 747-756.

[133] Pande V, Viswanathan V. Criteria and Considerations for the Selection of Redox Mediators in Nonaqueous Li–O2 Batteries[J]. ACS Energy Letters, 2017, 2(1): 60-63.

[134] Krishnamurthy D, Hansen H A, Viswanathan V. Universality in Nonaqueous Alkali Oxygen Reduction on Metal Surfaces: Implications for Li–O2 and Na–O2 Batteries[J]. ACS Energy Letters, 2016, 1(1): 162-168.

[135] Zhang T, Liao K, He P, et al. A self-defense redox mediator for efficient lithium–O 2 batteries[J]. Energy & Environmental Science, 2016, 9(3): 1024-1030.

[136] Kwak W-J, Hirshberg D, Sharon D, et al. Understanding the behavior of Li–oxygen cells containing LiI[J]. Journal of Materials Chemistry A, 2015, 3(16): 8855-8864.

[137] Xu J, Wu H-T, Wang X, et al. A new and environmentally benign precursor for the synthesis of mesoporous gC 3 N 4 with tunable surface area[J]. Physical Chemistry Chemical Physics, 2013, 15(13): 4510-4517.

[138] Zhang Y, Liu J, Wu G, et al. Porous graphitic carbon nitride synthesized via direct polymerization of urea for efficient sunlight-driven photocatalytic hydrogen production[J]. Nanoscale, 2012, 4(17): 5300-5303.

[139] Han Q, Wang B, Gao J, et al. Atomically thin mesoporous nanomesh of graphitic C3N4 for high-efficiency photocatalytic hydrogen evolution[J]. ACS nano, 2016, 10(2): 2745-2751.

[140] Zhang C, Lu Y, Jiang Q, et al. Synthesis of CdS hollow spheres coupled with g-C3N4 as efficient visible-light-driven photocatalysts[J]. Nanotechnology, 2016, 27(35): 355402.

[141] Chen X, Liu Q, Wu Q, et al. Incorporating Graphitic Carbon Nitride (g-C3N4) Quantum Dots into Bulk-Heterojunction Polymer Solar Cells Leads to Efficiency Enhancement[J]. Advanced Functional Materials, 2016.

[142] Ong W-J, Tan L-L, Ng Y H, et al. Graphitic carbon nitride (g-C3N4)-based photocatalysts for artificial photosynthesis and environmental remediation: are we a step closer to achieving sustainability?[J]. Chemical reviews, 2016, 116(12): 7159-7329.

[143] Zhou B, Guo L, Zhang Y, et al. A High-Performance Li–O2 Battery with a

Strongly Solvating Hexamethylphosphoramide Electrolyte and a LiPON-Protected Lithium Anode[J]. Advanced Materials, 2017.

[144] Wang Z L, Xu D, Xu J J, et al. Graphene Oxide Gel-Derived, Free-Standing, Hierarchically Porous Carbon for High-Capacity and High-Rate Rechargeable Li-O2 Batteries[J]. Advanced Functional Materials, 2012, 22(17): 3699-3705.

[145] Black R, Lee J H, Adams B, et al. The role of catalysts and peroxide oxidation in lithium–oxygen batteries[J]. Angewandte Chemie, 2013, 125(1): 410-414.

[146] Mitchell R R, Gallant B M, Shao-Horn Y, et al. Mechanisms of morphological evolution of Li2O2 particles during electrochemical growth[J]. The journal of physical chemistry letters, 2013, 4(7): 1060-1064.

[147] Horstmann B, Gallant B, Mitchell R, et al. Rate-dependent morphology of Li2O2 growth in Li–O2 batteries[J]. The journal of physical chemistry letters, 2013, 4(24): 4217-4222.

[148] Liu P, Cao Y L, Li G R, et al. A solar rechargeable flow battery based on photoregeneration of two soluble redox couples[J]. ChemSusChem, 2013, 6(5): 802-806.

[149] Bae J, Park Y J, Lee M, et al. Single-fiber-based hybridization of energy converters and storage units using graphene as electrodes[J]. Advanced materials, 2011, 23(30): 3446-3449.

[150] Yan N, Li G, Pan G, et al. TiN nanotube arrays as electrocatalytic electrode for solar storable rechargeable battery[J]. Journal of The Electrochemical Society, 2012, 159(11): A1770-A1774.

[151] Sun H, You X, Deng J, et al. A twisted wire-shaped dual-function energy device for photoelectric conversion and electrochemical storage[J]. Angewandte Chemie, 2014, 126(26): 6782-6786.

[152] Huang J, Jin Z, Xu Z-L, et al. Porous RuO2 nanosheet/CNT electrodes for DMSO-based Li-O2 and Li ion O2 batteries[J]. Energy Storage Materials, 2017, 8: 110-118.

[153] Zhang J, Sun B, Mcdonagh A M, et al. A multi-functional gel co-polymer bridging liquid electrolyte and solid cathode nanoparticles: An efficient route to Li–O2 batteries with improved performance[J]. Energy Storage Materials, 2017, 7: 1-7.

[154] Takechi K, Singh N, Arthur T S, et al. Decoupling Energy Storage from Electrochemical Reactions in Li–Air Batteries toward Achieving Continuous Discharge[J]. ACS Energy Letters, 2017, 2(3): 694-699.

[155] Liu R, Lei Y, Yu W, et al. Achieving Low Overpotential Lithium–Oxygen Batteries by Exploiting a New Electrolyte Based on N,N′-Dimethylpropyleneurea[J]. ACS Energy Letters, 2017, 2(2): 313-318.

[156] Armand M, Tarascon J M. Building better batteries[J]. Nature, 2008, 451(7179): 652-657.

[157] Guo S, Yi J, Sun Y, et al. Recent advances in titanium-based electrode materials for stationary sodium-ion batteries[J]. Energy & Environmental Science, 2016, 9(10): 2978-3006.

[158] Wang Y, Song Y, Xia Y. Electrochemical capacitors: mechanism, materials, systems, characterization and applications[J]. Chem Soc Rev, 2016, 45(21): 5925-5950.

[159] Grande L, Paillard E, Hassoun J, et al. The Lithium/Air Battery: Still an Emerging System or a Practical Reality?[J]. Advanced Materials, 2015, 27(5): 784-800.

[160] Baggetto L, Niessen R a H, Roozeboom F, et al. High Energy Density All-Solid-State Batteries: A Challenging Concept Towards 3D Integration[J]. Advanced

Functional Materials, 2008, 18(7): 1057-1066.

[161] Zhu X B, Zhao T S, Wei Z H, et al. A high-rate and long cycle life solid-state lithium-air battery[J]. Energy & Environmental Science, 2015, 8(12): 3745-3754.

[162] Li F, Tang D-M, Chen Y, et al. Ru/ITO: A Carbon-Free Cathode for Nonaqueous Li-O-2 Battery[J]. Nano Lett, 2013, 13(10): 4702-4707.

[163] Lu Y-C, Gasteiger H A, Shao-Horn Y. Catalytic Activity Trends of Oxygen Reduction Reaction for Nonaqueous Li-Air Batteries[J]. J Am Chem Soc, 2011, 133(47): 19048-19051.

[164] Peng Z, Freunberger S A, Chen Y, et al. A Reversible and Higher-Rate Li-O-2 Battery[J]. Science, 2012, 337(6094): 563-566.

[165] Yi J, Guo S, He P, et al. Status and prospects of polymer electrolytes for solid-state Li-O2 (air) batteries[J]. Energy & Environmental Science, 2017, 10(4): 860-884.

[166] Yi J, Wu S, Bai S, et al. Interfacial construction of Li2O2 for a performance-improved polymer Li-O2 battery[J]. Journal of Materials Chemistry A, 2016, 4(7): 2403-2407.

[167] Prabhakaran V, Mehdi B L, Ditto J J, et al. Rational design of efficient electrode–electrolyte interfaces for solid-state energy storage using ion soft landing[J]. Nature Communications, 2016, 7: 11399.

[168] Ohta N, Takada K, Zhang L, et al. Enhancement of the High-Rate Capability of Solid-State Lithium Batteries by Nanoscale Interfacial Modification[J]. Advanced Materials, 2006, 18(17): 2226-2229.

[169] Sakuda A, Hayashi A, Tatsumisago M. Interfacial Observation between LiCoO2 Electrode and Li2S−P2S5 Solid Electrolytes of All-Solid-State Lithium Secondary Batteries Using Transmission Electron Microscopy[J]. Chemistry of

Materials, 2010, 22(3): 949-956.

[170] Yu M Z, Ren X D, Ma L, et al. Integrating a redox-coupled dye-sensitized photoelectrode into a lithium-oxygen battery for photoassisted charging[J]. Nature Communications, 2014, 5.

[171] Liu Y, Li N, Wu S, et al. Reducing the charging voltage of a Li-O2 battery to 1.9 V by incorporating a photocatalyst[J]. Energy & Environmental Science, 2015, 8(9): 2664-2667.

[172] Liu Y, Li N, Liao K, et al. Lowering the charge voltage of Li–O 2 batteries via an unmediated photoelectrochemical oxidation approach[J]. Journal of Materials Chemistry A, 2016, 4(32): 12411-12415.

[173] Yu M Z, Mcculloch W D, Huang Z J, et al. Solar-powered electrochemical energy storage: an alternative to solar fuels[J]. Journal of Materials Chemistry A, 2016, 4(8): 2766-2782.

[174] Liu Y, Li N, Liao K M, et al. Lowering the charge voltage of Li-O-2 batteries via an unmediated photoelectrochemical oxidation approach[J]. Journal of Materials Chemistry A, 2016, 4(32): 12411-12415.

[175] Wu A P, Jing L Q, Wang J Q, et al. ZnO-dotted porous ZnS cluster microspheres for high efficient, Pt-free photocatalytic hydrogen evolution[J]. Scientific Reports, 2015, 5.

[176] Wu S, Zhu K, Tang J, et al. A long-life lithium ion oxygen battery based on commercial silicon particles as the anode[J]. Energy & Environmental Science, 2016, 9(10): 3262-3271.

[177] Wu A, Jing L, Wang J, et al. ZnO-dotted porous ZnS cluster microspheres for high efficient, Pt-free photocatalytic hydrogen evolution[J]. Scientific Reports, 2015, 5: 8858.

[178] Zhang J, Liu S, Yu J, et al. A simple cation exchange approach to Bi-doped ZnS hollow spheres with enhanced UV and visible-light photocatalytic H2-production activity[J]. Journal of Materials Chemistry, 2011, 21(38): 14655-14662.

[179] Hassoun J, Jung H-G, Lee D-J, et al. A Metal-Free, Lithium-Ion Oxygen Battery: A Step Forward to Safety in Lithium-Air Batteries[J]. Nano Lett, 2012, 12(11): 5775-5779.

[180] Wu S, Zhu K, Tang J, et al. A long-life lithium ion oxygen battery based on commercial silicon particles as the anode[J]. Energy & Environmental Science, 2016.

[181] Yi J, Zhou H. A Unique Hybrid Quasi-Solid-State Electrolyte for Li–O2 Batteries with Improved Cycle Life and Safety[J]. ChemSusChem, 2016, 9(17): 2391-2396.

[182] Yi J, Liu X, Guo S, et al. Novel Stable Gel Polymer Electrolyte: Toward a High Safety and Long Life Li–Air Battery[J]. Acs Applied Materials & Interfaces, 2015, 7(42): 23798-23804.

[183] Viswanathan V, Thygesen K S, Hummelshoj J S, et al. Electrical conductivity in Li2O2 and its role in determining capacity limitations in non-aqueous Li-O-2 batteries[J]. Journal Of Chemical Physics, 2011, 135(21).